

High-energy behavior of fermion-fermion scattering in a supersymmetric field theory*

Bing-Lin Young

Ames Laboratory—ERDA and Department of Physics, Iowa State University, Ames, Iowa 50011

T. F. Wong[†]

Serin Physics Laboratory, Rutgers, The State University, Piscataway, New Jersey 08854

J. W. Opoien

Ames Laboratory—ERDA and Department of Physics, Iowa State University, Ames, Iowa 50011

(Received 15 March 1976)

The high-energy behavior of the fermion-fermion and fermion-antifermion scattering amplitudes of a class of field theories, containing a spin-1/2 fermion field, a scalar field, and a pseudoscalar field, are investigated. These theories consist of a supersymmetric model, the Yukawa model, and the linear σ model. In the leading-logarithm approximation, ladders with fermions running along the sides in the t channel and mesons as rungs dominate in each order of two classes of diagrams. The sums of the dominant series give rise to fixed Regge cuts for all the three theories; the amplitude of the supersymmetric theory possesses a definite signature, while those of the other two lack it. A comparison of the result of the supersymmetric theory with the results of an asymptotically free theory and the spontaneously broken non-Abelian gauge theory is made.

I. INTRODUCTION

In the last decade and a half, we have witnessed the important role that quantum field theory has played in particle physics. Examples are numerous, such as the construction of algebra of currents,¹ the discovery of canonical anomalies,² the calculation of high-energy behavior of scattering amplitudes, Reggeization and eikonalization,³ the construction of a unified renormalizable theory of weak and electromagnetic interactions,⁴ the establishment of asymptotic freedom⁵ in non-Abelian gauge theory, and, more recently, the construction of supersymmetric theory.⁶ All of these contribute to our understanding of elementary-particle interactions. Especially, renormalizable non-Abelian gauge theories together with asymptotic freedom provide us with a theoretical basis for the understanding of Bjorken scaling⁷ and possibly quark confinement,⁸ and supersymmetry could be profoundly significant.

In the study of the high-energy behavior of scattering amplitudes the problem is centered on spontaneously broken non-Abelian gauge theory (SBNGT). McCoy and Wu,⁹ Nieh and Yao,¹⁰ and Tyburski¹¹ independently calculated, in the leading-logarithm approximation, the fermion-fermion scattering amplitude to sixth order. Despite the complicated structure of this type of theories, which makes an all-orders calculation extremely difficult, a very interesting cancellation of the transverse-momentum (P_\perp) integration occurs among the various diagrams of the same order. As a result, instead of being a $\ln^2 s$ series, as one would expect for a renormalizable theory, the series is one of $\ln s$ and the amplitude seems to

Reggeize, giving rise to a vector-meson trajectory. This agrees with the general result of Grisaru, Schnitzer, and Tsao.³ The surviving powers of $\ln s$ come from the longitudinal-momentum (P_L) integrations alone. The origin of this cancellation seems to be mysterious; its relation to gauge symmetry is not clear. Physically, the presence of P_\perp integration $\ln s$ signifies that the theory lacks P_\perp damping in particle-production amplitudes, contrary to experimental data of hadron productions. Hence the absence of $\ln s$ from P_\perp integration lends further credibility to SBNGT as a candidate for a theory of hadron interactions.

Another asymptotically free theory, ϕ^3 in six dimensions [$(\phi^3)_6$], has been studied by Brown, Gordon, Wong, and Young,¹² and by Muzinich and Tsao.¹³ They found that for the on-shell scattering amplitude, the leading-logarithm approximation gives rise to a $\ln^2 s$ series, seemingly not affected by asymptotic freedom. Nevertheless, in the deep-inelastic Regge region, asymptotic freedom does play an important role. As found by Lovelace¹⁴ and Cardy¹⁵ independently, the constraint of asymptotic freedom softens the kernel of the Bethe-Salpeter equation in $(\phi^3)_6$ and consequently modifies the asymptotic behavior of the amplitude. Lovelace¹⁶ also proposed a program to treat the class of asymptotically free theories, with the hope that the program may eventually be applied to non-Abelian gauge theory.

In order to gain further understanding of the general roles that symmetries may play in the asymptotic behavior of scattering amplitudes, we have investigated a supersymmetric theory. Common features of this type of theory and non-Abelian gauge theories are their high symmetries and the

effects of the symmetries on their renormalization.¹⁷ The particular version of the theory we shall study contains a Majorana spinor, a scalar, and a pseudoscalar. This theory is simple enough that no other symmetries will mask the issue, yet it possesses a sufficiently rich structure to provide a meaningful ground for the investigation.

In this paper, we shall concern ourselves with the questions of Reggeization and P_1 -integration cancellations in the supersymmetric model (s model) as mentioned above. We also compare the results with those of similar models without the supersymmetry—the Yukawa model (Y model) and the neutral version of the linear σ model. We find that two classes of diagrams, which can be summed up to all orders in the leading-logarithm approximation, dominate respectively the fermion-fermion and fermion-antifermion elastic scatterings. However, both classes contribute and dominate the fermion-fermion scattering in the s model, owing to the lack of fermion number conservation. The *two classes*, which have the same strength in each order and potentially could cancel each other in the leading term, *are in phase*. We find no P_1 -integration cancellations.

The plan of this paper is as follows: We begin in Sec. II by introducing a simple supersymmetric theory. Then we summarize briefly the Feynman diagram rules of the three models mentioned above. We also list all the final results in this section. Fourth-order diagrams are discussed in Sec. III, and sixth-order diagrams are discussed in Sec. IV. From the results of these two sections we determine the dominant classes of diagrams. Section V deals with the summation of these diagrams to all orders in the leading-logarithm approximation. Conclusions and discussion make up Sec. VI. Several relevant properties of the Majorana spinors are given in Appendix A. Appendixes B and C contain some of the essential formulas needed in Sec. V.

II. THE MODEL

We consider the simplest nontrivial model invariant under a supergauge transformation.¹⁸ It consists of a Majorana spinor field ψ ,¹⁹ a scalar field A , and a pseudoscalar field B . The Lagrangian density is

$$\begin{aligned} \mathcal{L}_s = & \frac{1}{2}[(\partial_\mu A)^2 - m^2 A^2] + \frac{1}{2}[(\partial_\mu B)^2 - m^2 B^2] \\ & + \frac{1}{2}(i\bar{\psi}\not{\partial}\psi - m\bar{\psi}\psi) - \frac{1}{2}g\bar{\psi}(A - i\gamma_5 B)\psi - \frac{1}{2}m g A(A^2 + B^2) \\ & - \frac{1}{8}g^2(A^2 + B^2)^2, \end{aligned} \quad (2.1)$$

where $\not{\partial} \equiv \gamma^\mu \partial_\mu$. The factor $\frac{1}{2}$ in front of the kinetic energy and mass terms of the spinor is due to the fact that ψ is self-conjugate; $\bar{\psi}$ and ψ are not in-

dependent. Note that all the masses are degenerate and that there is only one coupling constant. Except for these differences, the structure of this Lagrangian is similar to the neutral version of the linear σ model.²⁰

To define our notation, the Lagrangians of the Y model and the σ model are

$$\mathcal{L}_Y = \bar{\psi}(i\not{\partial} - m)\psi + \frac{1}{2}[(\partial_\mu \pi)^2 - \mu^2 \pi^2] + g\bar{\psi}i\gamma_5 \psi \pi \quad (2.2)$$

and

$$\begin{aligned} \mathcal{L}_\sigma = & \bar{\psi}(i\not{\partial} - m)\psi + \frac{1}{2}[(\partial_\mu \pi)^2 - \mu^2 \pi^2] + \frac{1}{2}[(\partial_\mu \sigma)^2 - \mu^2 \sigma^2] \\ & - g\bar{\psi}(\sigma + i\gamma_5 \pi)\psi - 4\lambda G\sigma(\sigma^2 + \pi^2) - \lambda G^2(\sigma^2 + \pi^2)^2 \\ & - 4\lambda\sigma^2 + \frac{1}{2}\mu_0^2(2G^{-1}\sigma + \sigma^2 + \pi^2), \end{aligned} \quad (2.3)$$

where σ and π are respectively the scalar and pseudoscalar fields, and $G = g/m$. The last two terms in Eq. (2.3) are needed for renormalization; they do not concern us here. The Feynman rules for the three theories are summarized in the diagrams of Fig. 1. We use a dashed line for the propagator of $B(\pi)$, a wavy line for $A(\sigma)$, and a solid line for ψ . Only diagrams (a), (b), (c), and (e) are relevant to \mathcal{L}_Y . Diagrams (a)–(i) apply to both \mathcal{L}_s and \mathcal{L}_σ . Diagram (j) applies to \mathcal{L}_σ only. When rules of the two models are associated with different factors, the ones in the brackets are applicable to \mathcal{L}_σ .

It is worth pointing out that the real difference between the s model and the σ model at high energy

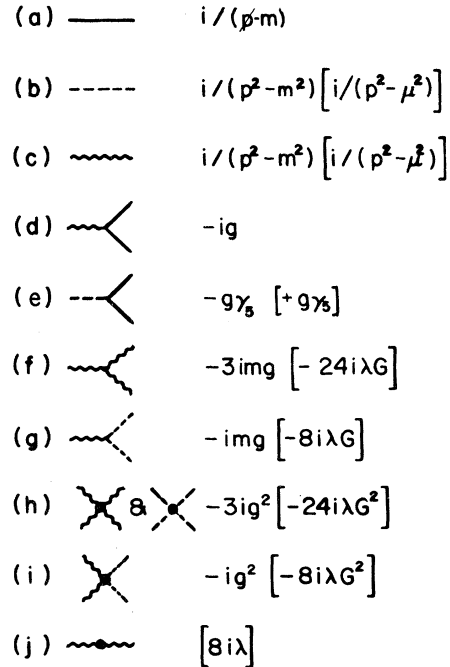


FIG. 1. Feynman rules for the s , Y , and σ models (see text).

is the lack of fermion number in the former, since the mass difference will not enter (except as a scale factor) and only the coupling for $\psi-\bar{\psi}-A(\sigma)$ and $\psi-\bar{\psi}-B(\pi)$ enters the leading-logarithm approximation.

Before presenting the details of the calculation in the next three sections, let us list all the final results of the spin-averaged scattering amplitudes in the three models. They will also appear at the end of Sec. V.

(a) *The s model.* The leading-logarithmic approximations of the u diagrams and s diagrams (see Sec. III for definition) are

$$T_u = -ig^2 \sum_{n=0}^{\infty} \frac{1}{n!(n+1)!} (\bar{g}^2 \ln^2 s)^n$$

$$\simeq \frac{-ig^2}{\sqrt{4\pi}} \frac{s^{2\bar{g}}}{(\bar{g} \ln s)^{3/2}} \quad (2.4)$$

and

$$T_s = -ig^2 \sum_{n=0}^{\infty} \frac{1}{n!(n+1)!} [\bar{g}^2 (\ln s - i\pi)^2]^n$$

$$\simeq \frac{-ig^2}{\sqrt{4\pi}} e^{-i2\pi\bar{g}} \frac{s^{2\bar{g}}}{(\bar{g} \ln s)^{3/2}}, \quad (2.5)$$

where

$$\bar{g}^2 = g^2/8\pi^2.$$

The scattering amplitude is

$$T = T_u + T_s$$

$$\simeq \frac{-ig^2}{\sqrt{4\pi}} (1 + e^{-i2\pi\bar{g}}) \frac{s^{2\bar{g}}}{(\bar{g} \ln s)^{3/2}}. \quad (2.6)$$

(b) *The σ model.* The fermion-fermion and fermion-antifermion scattering amplitudes are respectively given by T_u and T_s , i.e., Eqs. (2.4) and (2.5).

(c) *The Y model.* The amplitudes are similar to the corresponding amplitudes of the σ model with, however, g^2 and \bar{g}^2 replaced by $g^2/2$ and $\bar{g}^2/2$.

III. THE FOURTH-ORDER DIAGRAMS

We consider the fermion-fermion scattering. The notation is defined in Fig. 2. There the momenta are given by

$$P_a = (E, 0, 0, P),$$

$$P_b = (E, 0, 0, -P), \quad (3.1)$$

$$r = (0, r_x, r_y, 0).$$

As usual, we define $s = (P_a + P_b)^2$, $t = 4r^2$, and $u = (P_a - P_b)^2$. We are interested in the asymptotic behavior of the scattering amplitude $s \rightarrow \infty$ with t fixed and finite.

In the Y model and the σ model, there are two classes of diagrams in each order which we refer

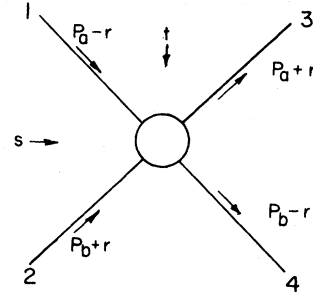


FIG. 2. Momentum assignments for the general two-body scattering amplitudes.

to as the t diagrams and the u diagrams (see Fig. 3). In the former mesons are exchanged in the t channel and in the latter mesons are exchanged in the u channel. Because of the lack of fermion number conservation, another class of diagrams, corresponding to annihilation in the Y and σ models, contribute to the s model. This third class, with mesons exchanged in the s channel, will be called the s diagrams. The three types of diagrams are obtainable from each other in the usual way: u diagrams can be obtained from t diagrams by crossing the two outgoing fermions; crossing one initial and one final fermion, say labeled by 2 and 4 (see Fig. 2), of a u diagram gives an s diagram. This also determines their relative signs: the s and t diagrams have the same sign, and the u diagrams have the opposite sign. All the calculations will be done in the s model; the final results for the fermion-fermion and fermion-antifermion scatterings in the Y and σ models can

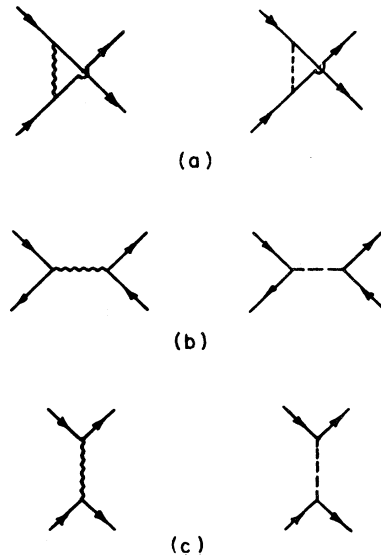


FIG. 3. Born diagrams: (a) u diagrams, (b) s diagrams, (c) t diagrams.

be obtained straightforwardly with simple modification, which we shall discuss later.

Because of the lack of fermion number, either u or v spinors can be used, as they are related by the charge conjugation matrix. For definiteness, we shall use u spinors in the t and u diagrams, but both spinors in the s diagram (see Appendix A). The arrows associated with the external fermion lines denote conventionally the use of u or v spinors. The external momentum flows are always from the left to the right as depicted in Fig. 2.

Let us mention in passing that there are six diagrams in the second order as shown in Fig. 3. They all go like a constant for $s \rightarrow \infty$. Using the obvious notation $T_s^{(n)}$, $T_u^{(n)}$, and $T_t^{(n)}$ to denote amplitudes of the three classes of diagrams of order $2n$, we have

$$T_s^{(1)} \approx -ig^2 \delta_{\lambda_1 \lambda_2} \delta_{\lambda_3 \lambda_4} (1 + \delta_{\lambda_1, \lambda_2} - \delta_{\lambda_1, -\lambda_3}), \quad (3.2a)$$

$$T_u^{(1)} \approx -ig^2 [1 - (\delta_{\lambda_1, +} - \delta_{\lambda_1, -})(\delta_{\lambda_2, +} - \delta_{\lambda_2, -})], \quad (3.2b)$$

with

$$\lambda_1 \neq \lambda_4 \text{ and } \lambda_2 \neq \lambda_3,$$

where λ_j is the helicity of particle $j=1, 2, 3$, and 4. $T_t^{(1)}$ is rather complicated and unilluminating; we shall not give it here. Examples of the spinor wave functions in the infinite-momentum frame, needed for obtaining the above expressions, are given in Appendix A.

Fourth order contains 24 box diagrams and many second-order radiative corrections to the Born terms. As will be shown in the following, the leading terms behave like $\ln^2 s$, hence the radiative correction diagrams (of order $\ln s$) are

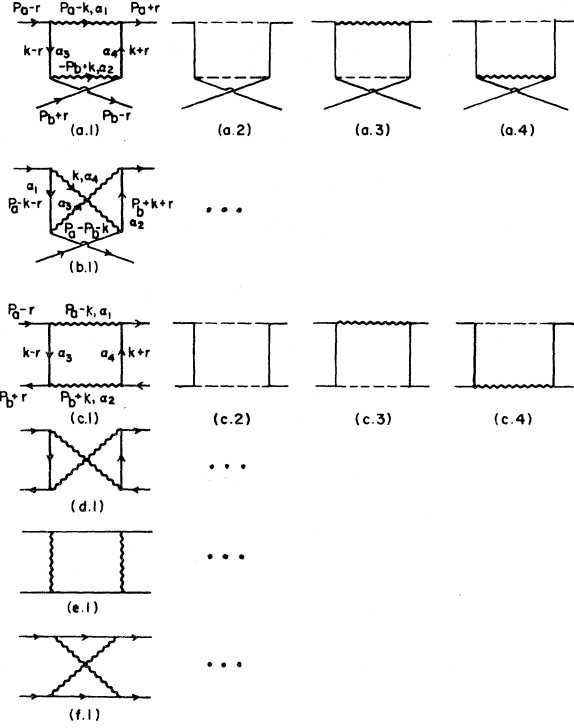


FIG. 4. Fourth-order box diagrams: (a) and (b) u diagrams, (c) and (d) s diagrams, (e) and (f) t diagrams. The arrows associated with the external fermion lines indicate the use of u or v spinors. The external momenta flows are always from the left to the right.

obviously nondominant; they will not be discussed further. The box diagrams are given in Fig. 4. We shall evaluate their asymptotic behavior by means of the Feynman parameter technique.²¹

Diagrams 4(a.1)–4(a.4). First we evaluate 4(a.1) and 4(a.2),²²

$$T_a^{(2)} = -(-ig)^4 i^4 \int_k N_a^{(2)} / D_a^{(2)}, \quad (3.3)$$

where

$$\begin{aligned} N_a^{(2)} &= \bar{u}(P_a + r)(\not{k} + \not{r} + m)u(P_b + r)\bar{u}(P_b - r)(\not{k} - \not{r} + m)u(P_a - r) \\ &\quad + \bar{u}(P_a + r)i\gamma_5(\not{k} + \not{r} + m)i\gamma_5 u(P_b + r)\bar{u}(P_b - r)i\gamma_5(\not{k} - \not{r} + m)i\gamma_5 u(P_b - r) \\ &= 2t_{\mu\nu}T^{\mu\nu} + 2m^2\tilde{N}_a, \end{aligned} \quad (3.4a)$$

$$t_{\mu\nu} = \bar{u}(P_a + r)\gamma_\mu u(P_b + r)\bar{u}(P_b - r)\gamma_\nu u(P_a - r), \quad (3.4b)$$

$$T^{\mu\nu} = (k + r)^\mu (k - r)^\nu, \quad (3.4c)$$

$$\tilde{N}_a = \bar{u}(P_a + r)u(P_b + r)\bar{u}(P_b - r)u(P_a - r). \quad (3.5)$$

The denominator is (see Fig. 4 for notation)

$$\begin{aligned} D_a^{(2)} &= [(P_a - k)^2 - m^2][(P_b - k)^2 - m^2][(k + r)^2 - m^2][(k - r)^2 - m^2] \\ &= 3! \int_0^1 d\alpha_1 d\alpha_2 d\alpha_3 d\alpha_4 \delta\left(1 - \sum_{i=1}^4 \alpha_i\right) \frac{1}{\tilde{D}_a^4}, \end{aligned} \quad (3.6)$$

where

$$\begin{aligned}\bar{D}_a &= \alpha_1[(P_a - k)^2 - m^2] + \alpha_2[(P_b - k)^2 - m^2] + \alpha_3[(k - r)^2 - m^2] + \alpha_4[(k + r)^2 - m^2] \\ &= (k - G_a)^2 - \Delta_a,\end{aligned}\quad (3.7a)$$

$$\Delta_a = m^2[1 - (\alpha_1 + \alpha_2) + (\alpha_1 - \alpha_2)^2] + \tilde{r}^2[\alpha_3 + \alpha_4 - \alpha_1 - \alpha_2 + (\alpha_1 - \alpha_2)^2 - (\alpha_3 - \alpha_4)^2] + \alpha_1\alpha_2 s - i\epsilon,\quad (3.7b)$$

$$G_a = \alpha_1 P_a + \alpha_2 P_b + (\alpha_3 - \alpha_4)r.\quad (3.7c)$$

The contribution of the first term of (3.4a) is

$$t_{\mu\nu} \int_k \frac{T^{\mu\nu}}{D_a^{(2)}} = \frac{i\pi^2}{(2\pi)^4} \int d\alpha_1 d\alpha_2 d\alpha_3 d\alpha_4 \delta\left(1 - \sum \alpha_j\right) t_{\mu\nu} \left[-\frac{g^{\mu\nu}}{2\Delta_a} + (G+r)^\mu (G-r)^\nu \frac{1}{\Delta_a^2} \right].\quad (3.8)$$

Using the standard notation, $\gamma_\pm = \gamma^0 \pm \gamma^3$ and $\tilde{\gamma}_\pm = (\gamma^1, \gamma^2)$, we have

$$\begin{aligned}g^{\mu\nu} t_{\mu\nu} &= \bar{u}(P_a + r)\gamma_\mu u(P_b + r) \bar{u}(P_b - r)\gamma^\mu u(P_a - r) \\ &= \frac{1}{2} \bar{u}(P_a + r)\gamma_+ u(P_b + r) \bar{u}(P_b - r)\gamma_- u(P_a - r) + \frac{1}{2} \bar{u}(P_a + r)\gamma_- u(P_b + r) \bar{u}(P_b - r)\gamma_+ u(P_a - r) \\ &\quad - \bar{u}(P_a + r)\tilde{\gamma}_\perp u(P_b + r) \bar{u}(P_b - r)\tilde{\gamma}_\perp u(P_a - r) \\ &= -2s \delta_{\lambda_1 \lambda_3} \delta_{\lambda_2 \lambda_4} \delta_{\lambda_1 \lambda_2} + O(1).\end{aligned}\quad (3.9)$$

The leading term comes from the γ_\perp components. The second term in (3.8) gives

$$t_{\mu\nu} (G+r)^\mu (G-r)^\nu = O(s).\quad (3.10)$$

Substituting (3.9) and (3.10) into (3.8), we obtain its leading term

$$i\pi^2/(2\pi)^4 \frac{\ln^2 s}{2} \delta_{\lambda_1 \lambda_3} \delta_{\lambda_2 \lambda_4} \delta_{\lambda_1 \lambda_2}.$$

Equation (3.9) dominates, while (3.10) gives a lns contribution. The term proportional to \tilde{N}_a , Eq. (3.4a), also gives rise to a lns term. Collecting the above results, we have

$$T_a'^{(2)} = -i g^2 \left(\frac{g}{4\pi}\right)^2 \ln^2 s \delta_{\lambda_1 \lambda_3} \delta_{\lambda_2 \lambda_4} \delta_{\lambda_1 \lambda_2}.\quad (3.11)$$

Diagrams 4(a.3) and 4(a.4) can be evaluated similarly. We write

$$T_a''^{(2)} = -(-ig)^4 i^4 \int_k N_a'^{(2)}/D_a^{(2)},\quad (3.12)$$

where $D_a^{(2)}$ is given by (3.6) and

$$\begin{aligned}N_a'^{(2)} &= \bar{u}(P_a + r)(\not{k} + \not{r} + m) i\gamma_5 u(P_b + r) \bar{u}(P_b - r) i\gamma_5 (\not{k} - \not{r} + m) u(P_a - r) \\ &\quad + \bar{u}(P_a + r) i\gamma_5 (\not{k} + \not{r} + m) u(P_b + r) \bar{u}(P_b - r) (\not{k} - \not{r} + m) i\gamma_5 u(P_a - r).\end{aligned}\quad (3.13)$$

Making a similar decomposition as (3.4a) and following the same procedure, we find that the term corresponding to (3.9) dominates:

$$g^{\mu\nu} \bar{u}(P_a + r)\gamma_\mu \gamma_5 u(P_b + r) \bar{u}(P_b - r)\gamma_\nu \gamma_5 u(P_a - r) = -2s \delta_{\lambda_1 \lambda_4} \delta_{\lambda_2 \lambda_3} \delta_{\lambda_1 \lambda_2} + O(1),\quad (3.14)$$

which is identical to (3.9) and also arises from the $\tilde{\gamma}_\perp$ terms. Now the total contribution to diagrams (a.1)–(a.4) is

$$T_a^{(2)} = T_a''^{(2)} + T_a'^{(2)} = -2i g^2 \left(\frac{g}{4\pi}\right)^2 \ln^2 s \delta_{\lambda_1 \lambda_3} \delta_{\lambda_2 \lambda_4} \delta_{\lambda_1 \lambda_2}.\quad (3.15)$$

Despite the fact that particles 1 and 3, 2 and 4 are not directly connected with each other, helicities are still conserved from 1 to 3 and 2 to 4. Further, helicities of all the particles are the same for the leading term.

Diagrams 4(b.1)–4(b.2). These can be treated similarly. The Feynman parametrization of the denominators is of the form

$$\begin{aligned}\{k - [(\alpha_1 + \alpha_4)P_a - (\alpha_2 + \alpha_4)P_b - (\alpha_1 + \alpha_2)r]\}^2 - \Delta_b, \\ \Delta_b = m^2[1 - \alpha_1 - \alpha_2 - 4\alpha_3 + (\alpha_1 + \alpha_2 + 2\alpha_3)^2] - \tilde{r}^2(4\alpha_3\alpha_4) + s[\alpha_3 - (\alpha_1 + \alpha_3)(\alpha_2 + \alpha_3)] - i\epsilon.\end{aligned}\quad (3.16)$$

Since the γ_\perp components dominate as stated before, the numerators are proportional to s . We note that diagrams 4(a.1)–4(a.4) are planar and that 4(b.1) and 4(b.2) are nonplanar, as their figures suggest. Following Tiktopoulos,²¹ we find that these latter diagrams behave at most like lns.

The amplitude of the u diagrams is given by $T_u^{(2)}$,

$$T_u^{(2)} = -i2 \frac{1}{2!} g^2 \bar{g}^2 \ln^2 s \delta_{\lambda_1 \lambda_3} \delta_{\lambda_2 \lambda_4} \delta_{\lambda_1 \lambda_2}, \quad (3.17)$$

where

$$\bar{g}^2 = g^2 / 8\pi^2. \quad (3.18)$$

Diagrams 4(c.1)–4(c.4) and 4(d.1)–4(d.4). The calculation here is parallel to that of 4(a.1)–4(a.4). We shall mention the steps briefly. Diagrams 4(c.1) and 4(c.2) give

$$T_c'^{(2)} = (-ig)^2 (i)^4 \int_k N_c^{(2)} / D_c^{(2)}, \quad (3.19)$$

where

$$\begin{aligned} N_c^{(2)} &\equiv \bar{u}(P_a + r)(\not{k} + \not{r} + m)v(P_b - r)\bar{v}(P_b + r)(\not{k} - \not{r} + m)u(P_a - r) \\ &\quad + \bar{u}(P_a + r)i\gamma_5(\not{k} + \not{r} + m)i\gamma_5 v(P_b - r)\bar{v}(P_b + r)i\gamma_5(\not{k} - \not{r} + m)i\gamma_5 u(P_a - r) \\ &= 2t'_{\mu\nu} T'^{\mu\nu} + 2m^2 \tilde{N}_c \end{aligned} \quad (3.20)$$

and

$$t'_{\mu\nu} \equiv \bar{u}(P_a + r)\gamma_\mu v(P_b - r)\bar{v}(P_b + r)\gamma_\nu u(P_a - r), \quad (3.21a)$$

$$T'^{\mu\nu} \equiv (k + r)^\mu (k - r)^\nu, \quad (3.21b)$$

$$\tilde{N}_c \equiv \bar{u}(P_a + r)v(P_b - r)\bar{v}(P_b + r)u(P_a - r). \quad (3.21c)$$

The denominator is

$$D_c = 3! \int d\alpha_1 d\alpha_2 d\alpha_3 d\alpha_4 \frac{1}{D_c^4} \delta\left(1 - \sum \alpha_j\right), \quad (3.22a)$$

$$\tilde{D}_c = \{k - [\alpha_1 P_a - \alpha_2 P_b + (\alpha_3 - \alpha_4)r]\}^2 - \Delta_c, \quad (3.22b)$$

$$\Delta_c \equiv m^2[1 - (\alpha_1 + \alpha_2) + (\alpha_1 + \alpha_2)^2] - \tilde{r}^2[\alpha_1 + \alpha_2 - \alpha_3 - \alpha_4 - (\alpha_1 + \alpha_2)^2 + (\alpha_3 - \alpha_4)^2] - s\alpha_1\alpha_2 - i\epsilon. \quad (3.22c)$$

After the k integration, we find that the dominant term is given by

$$g^{\mu\nu} t'_{\mu\nu} = -2s \delta_{\lambda_1 \lambda_3} \delta_{\lambda_2 \lambda_4} \delta_{\lambda_1, -\lambda_2} + O(1),$$

which again comes from the γ_\perp components. Then

$$\begin{aligned} T_c'^{(2)} &= -ig^2 (g/4\pi)^2 (\ln s - i\pi)^2 \\ &\quad \times \delta_{\lambda_1 \lambda_3} \delta_{\lambda_2 \lambda_4} \delta_{\lambda_1, -\lambda_2}. \end{aligned} \quad (3.23)$$

Diagrams 4(c.3) and 4(c.4) give exactly the same result.

Diagrams 4(d.1)–4(d.4) are nonleading and behave like lns. Summarizing the above result, we have

$$\begin{aligned} T_s^{(2)} &= T_c^{(2)} = 2T_c'^{(2)} \\ &= -i2 \frac{g^2}{2!} \bar{g}^2 (\ln s - i\pi)^2 \delta_{\lambda_1 \lambda_3} \delta_{\lambda_2 \lambda_4} \delta_{\lambda_1, -\lambda_2}. \end{aligned} \quad (3.24)$$

Notice that $T_u^{(2)}$ and $T_s^{(2)}$, Eqs. (3.17) and (3.24), have different helicity structure. Recall that their Feynman amplitudes have opposite signs. How-

ever, a negative sign results in $T_s^{(2)}$ because of the sign of the s term in Δ_c . This compensation of the sign in the s and u diagrams holds also in all higher orders, so that their leading terms are always in phase.

Diagrams 4(e.1)–4(e.4) and 4(f.1)–4(f.4). It turns out that these sets of diagrams behave like lns. What happens can be described briefly as follows. The dominant contributions to the numerators are from γ_\perp . Then both of the terms, which are similar to the two terms in Eq. (3.8), behave like $\ln^2 s$; they cancel each other, so that $T_i^{(2)} \sim \ln s$. This result can easily be obtained if one considers the forward spin-averaged amplitude.

Let us summarize the corresponding results of the Y and σ models. The u diagrams dominate the fermion-fermion scattering and the s diagrams dominate the fermion-antifermion scattering. The asymptotic amplitudes are given respectively by $\frac{1}{4}T_u^{(2)}$ and $\frac{1}{4}T_s^{(2)}$ in the Y model and by $T_u^{(2)}$ and $T_s^{(2)}$ in the σ model. The mass differences in these models do not show up in the leading behavior of

the amplitudes.

We conclude this section by comparing our results with the similar amplitude of quantum electrodynamics. There, the diagram like 4(e.1) dominates, while the diagram like 4(a.1) is suppressed by a factor $1/s$. This fact, which holds true in higher orders, agrees with the conjecture made by Chang and Ma,²³ based on their quantum-electrodynamics calculation in the infinite-momentum frame, that amplitudes are dominated by the highest-spin exchanges in the crossed channel.

IV. SIXTH-ORDER DIAGRAMS

In this section, we study the high-energy behavior of the sixth-order diagrams. The planar diagrams, eight each in the s and u classes and 16 in the t class, are shown in Figs. 5 and 6, respectively. In addition, there are many more: nonplanar diagrams, diagrams involving quartic vertices, radiative corrections of the lower-order diagrams (containing many meson triple

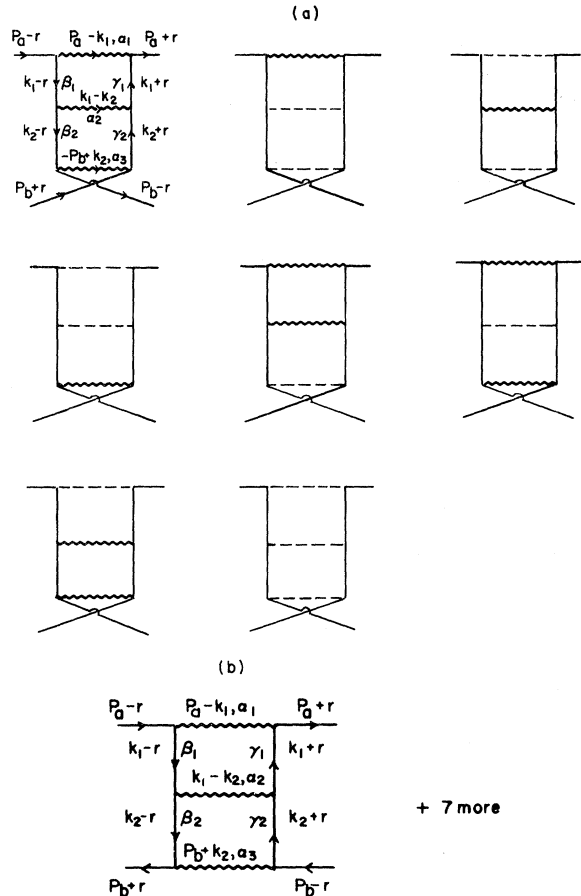


FIG. 5. Sixth-order diagrams: (a) u diagrams, (b) s diagrams.

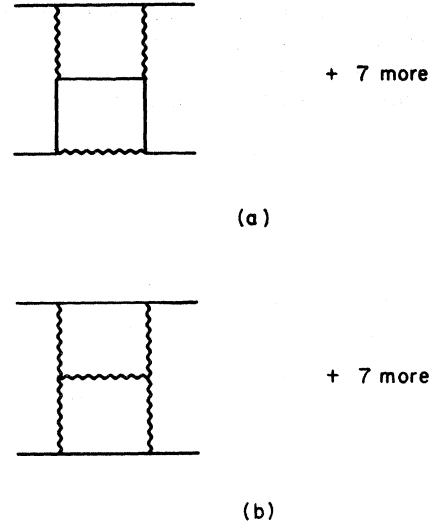


FIG. 6. Sixth-order t diagrams.

vertices), etc. We shall concern ourselves primarily with the planar diagrams given in Fig. 5. All the other diagrams will be discussed briefly at the end of this section.

The evaluation of these diagrams is rather tedious owing to the presence of the spinors and the γ matrices. In the following, we present the essential steps, using the standard parameter space method.²¹

Consider the first four u diagrams in Fig. 5(a), which we write as

$$T_a^{(3)} = -(-ig)^6 i^7 \int_{k_1} \int_{k_2} N_a^{(3)} / D_a^{(3)}. \quad (4.1)$$

After simplification, the numerator is

$$N_a^{(3)} = 4N_{a1}^{(3)} + 4m^2 N_{a2}^{(3)} + 4m^4 N_{a3}^{(3)}, \quad (4.2)$$

where

$$\begin{aligned} N_{a1}^{(3)} &= \bar{u}(P_a + r)(\not{k}_1 + \not{r})(\not{k}_2 + \not{r})u(P_b + r) \\ &\quad \times \bar{u}(P_b - r)(\not{k}_2 - \not{r})(\not{k}_1 - \not{r})u(P_a - r), \\ N_{a2}^{(3)} &= \bar{u}(P_a + r)(\not{k}_1 + \not{r})u(P_b + r)\bar{u}(P_b - r)(\not{k}_1 - \not{r}) \\ &\quad \times u(P_a - r) + (k_1 \leftrightarrow k_2), \\ N_{a3}^{(3)} &= \bar{u}(P_a + r)u(P_b + r)\bar{u}(P_b - r)u(P_a - r). \end{aligned}$$

$N_{a1}^{(3)}$ gives the dominant contribution. We rewrite it as

$$N_{a1}^{(3)} \equiv t_{\mu\nu\lambda\rho} T^{\mu\nu\lambda\rho}, \quad (4.3a)$$

where

$$t_{\mu\nu\lambda\rho} = \bar{u}(P_a + r)\gamma_\mu\gamma_\nu u(P_b + r)\bar{u}(P_b - r)\gamma_\lambda\gamma_\rho u(P_a - r), \quad (4.3b)$$

$$T^{\mu\nu\lambda\rho} = (k_1 + r)^\mu (k_2 + r)^\nu (k_2 - r)^\lambda (k_1 - r)^\rho. \quad (4.3c)$$

The denominator in (4.1) is

$$D_a^{(3)} = 6! \int d\alpha_1 d\alpha_2 d\alpha_3 d\beta_1 d\beta_2 d\gamma_1 d\gamma_2 \left(\frac{1}{\bar{D}_a^{(3)}} \right)^7 \\ \times \delta \left(1 - \sum \alpha_j - \sum \beta_j - \sum \gamma_j \right), \quad (4.4)$$

where

$$\bar{D}_a^{(3)} = k^T A K - 2K^T B P - \sigma, \\ K = \begin{pmatrix} k_1 \\ k_2 \end{pmatrix}, \quad P = \begin{pmatrix} P_a \\ P_b \\ r \end{pmatrix}, \\ A = \begin{pmatrix} \eta_1 & -\alpha_2 \\ -\alpha_2 & \eta_2 \end{pmatrix}, \quad B = \begin{pmatrix} \alpha_1 & 0 & \beta_1 - \gamma_1 \\ 0 & \alpha_3 & \beta_2 - \gamma_2 \end{pmatrix}, \quad (4.5)$$

$$\eta_1 = \alpha_1 + \alpha_2 + \beta_1 + \gamma_1, \quad \eta_2 = \alpha_2 + \alpha_3 + \beta_2 + \gamma_2, \\ \sigma = m^2(1 - \alpha_1 - \alpha_3) + \bar{r}^2(1 - 2\alpha_1 - 2\alpha_3 - \alpha_2) - i\epsilon, \\ \bar{C} \equiv \det A = \eta_1 \eta_2 - \alpha_2^2.$$

Let us change the integration variables

$$k = Rk' + A^{-1}Bp, \quad (4.6)$$

where $K' = \begin{pmatrix} k'_1 \\ k'_2 \end{pmatrix}$ and $R \equiv \begin{pmatrix} R_{11} & R_{12} \\ R_{21} & R_{22} \end{pmatrix}$. Then

$$\bar{D}_a^{(3)} = K'^T R^T A R K' - (BP)^T A^{-1}(BP) - \sigma. \quad (4.7)$$

R is chosen to diagonalize A so that

$$R^T A R = \begin{pmatrix} \lambda_1 & 0 \\ 0 & \lambda_2 \end{pmatrix}, \quad \bar{C} = \lambda_1 \lambda_2. \quad (4.8)$$

One can show that

$$\Delta_a \bar{C} \equiv \bar{C} \sigma + \bar{C} (BP)^T A^{-1}(BP) \\ = m^2 f_m - \bar{r}^2 f_r + \alpha_1 \alpha_2 \alpha_3 S, \quad (4.9a)$$

$$T^{\mu\nu\lambda\rho} \simeq (k'_1 + G_1 + r)^\mu (k'_2 + G_2 + r)^\nu (k'_2 + G_2 - r)^\lambda (k'_1 + G_1 - r)^\rho.$$

Substituting (4.3), (4.4), and (4.7)–(4.10) into (4.1), we get

$$T_a'^{(3)} = -i g^6 4\pi^2 \left(\frac{1}{2\pi} \right)^8 \int d\alpha_1 d\alpha_2 d\alpha_3 d\beta_1 d\beta_2 d\gamma_1 d\gamma_2 \delta \left(1 - \sum \alpha_j - \sum \beta_j - \sum \gamma_j \right) \\ \times \frac{1}{\bar{C}^2} \left[\frac{1}{2} g^{\mu\rho} g^{\nu\lambda} \frac{1}{\bar{C} \Delta_a} - (\beta_1 + \gamma_1) g^{\nu\lambda} (G_1 + r)^\mu (G_1 - r)^\rho \frac{1}{2\bar{C} \Delta_a^2} \right. \\ \left. - (\beta_2 + \gamma_2) g^{\mu\rho} (G_2 + r)^\nu (G_2 - r)^\lambda \frac{1}{2\bar{C} \Delta_a^2} \right. \\ \left. + (G_1 + r)^\mu (G_1 - r)^\rho (G_2 + r)^\nu (G_2 - r)^\lambda \frac{2}{\Delta_a^3} \right] t_{\mu\nu\lambda\rho}. \quad (4.11)$$

The first term in the bracket [] gives the dominant contribution, and

$$g^{\mu\rho} g^{\nu\lambda} t_{\mu\nu\lambda\rho} = 4s \delta_{\lambda_1 \lambda_3} \delta_{\lambda_2 \lambda_4} \delta_{\lambda_1, -\lambda_2} + O(1), \quad (4.12)$$

which comes from the $\gamma_1 \gamma'_1$ components. The procedure for the evaluation of the integral

$$\int d\alpha_1 d\alpha_2 d\alpha_3 d\beta_1 d\beta_2 d\gamma_1 d\gamma_2 \delta \left(1 - \sum \alpha_j - \sum \beta_j - \sum \gamma_j \right) \frac{1}{\bar{C}^2} \frac{1}{\Delta_a \bar{C}} \quad (4.13a)$$

has been discussed in detail in Ref. 12; we give only the result:

where

$$f_m = \bar{C}(1 - \alpha_1 - \alpha_3) + \alpha_1^2 \eta_2 + \alpha_3^2 \eta_1 - 2\alpha_1 \alpha_2 \alpha_3, \quad (4.9b)$$

$$f_r = -\bar{C}(1 - 2\alpha_1 - 2\alpha_3 - \alpha_2) \\ + 2\alpha_2(\beta_1 - \gamma_1)(\beta_2 - \gamma_2) + \eta_2(\beta_1 - \gamma_1)^2 \\ + \eta_1(\beta_2 - \gamma_2)^2 - \alpha_1^2 \eta_2 - \alpha_3^2 \eta_1 + 2\alpha_1 \alpha_2 \alpha_3. \quad (4.9c)$$

It is not necessary to know the elements R_{11} , etc. of R ; they enter the calculation always in the following combinations:

$$R_{11} R_{22} - R_{12} R_{21} = 1, \\ R_{11}^2 \lambda_2 + R_{12}^2 \lambda_1 = \eta_2, \\ R_{22}^2 \lambda_1 + R_{21}^2 \lambda_2 = \eta_1, \\ \lambda_2 R_{11} R_{21} + \lambda_1 R_{12} R_{22} = \alpha_2.$$

We have performed the calculation in the full complication indicated above. However, the matter can be simplified, if we put $\alpha_1 = \alpha_2 = \alpha_3 = 0$ in the numerator, i.e., $N_a^{(3)}$. This is permissible, since $\alpha_1 = \alpha_2 = \alpha_3 = 0$ is part of the domain contributing to the leading logarithm. In this approximation, A is diagonalized and R reduces to the unit matrix. Let us emphasize that this approximation is only applied to the *numerator*, e.g., in $T^{\mu\nu\lambda\rho}$. Bearing this in mind, we substitute K with $K' + G$ in $T^{\mu\nu\lambda\rho}$, where G is obtained from $A^{-1}BP$ by setting $\alpha_1 = \alpha_2 = \alpha_3 = 0$:

$$G = \frac{1}{\bar{C}} \begin{pmatrix} (\beta_2 + \gamma_2)(\beta_1 - \gamma_1)r \\ (\beta_1 + \gamma_1)(\beta_2 - \gamma_2)r \end{pmatrix} \equiv \begin{pmatrix} G_1 \\ G_2 \end{pmatrix}. \quad (4.10)$$

Then

$$\frac{2}{4!} \frac{1}{s} \ln^4 s. \quad (4.13b)$$

Now the evaluation of (4.1) is completed:

$$T_a'^{(3)} = -i \frac{g^6}{2^7 \pi^4} \frac{1}{3!} \ln^4 s \delta_{\lambda_1 \lambda_3} \delta_{\lambda_2 \lambda_4} \delta_{\lambda_1, -\lambda_2}. \quad (4.14)$$

The last four diagrams in Fig. 5(a) have the same denominator. The dominant numerator is similar to (4.3a) with $t_{\mu\nu\lambda\rho}$ replaced by

$$t'_{\mu\nu\lambda\rho} = \bar{u}(P_a + r) i \gamma_5 \gamma_\mu \gamma_\nu u(P_b + r) \bar{u}(P_b - r) \gamma_\lambda \gamma_\rho i \gamma_5 u(P_a - r). \quad (4.15)$$

Following the same procedure as illustrated above, we obtain an expression similar to (4.11) with $t_{\mu\nu\lambda\rho}$ replaced by $t'_{\mu\nu\lambda\rho}$, (4.15). The leading contribution is the same as (4.14). Adding the two results we have

$$\begin{aligned} T_u^{(3)} &\approx 2T_a'^{(3)} \\ &\approx -i 2 \frac{g^2}{2!3!} \bar{g}^4 \ln^4 s \delta_{\lambda_1 \lambda_3} \delta_{\lambda_2 \lambda_4} \delta_{\lambda_1, -\lambda_2}, \end{aligned} \quad (4.16)$$

where \bar{g} is defined in (3.18). We see that the helicity is again conserved.

But $T_u^{(3)}$ has different helicity structure from $T_u^{(2)}$; it has the same helicities as the fourth-order s diagrams. Let us remark that in the case of the spin-averaged amplitude, this distinction between the two orders disappears. This remark also applies to the s diagrams to be discussed next.

Next we consider the s diagrams which are given in Fig. 5(b). The first four diagrams are denoted by

$$T_b'^{(3)} = (-ig)^6 (i)^7 6! \int d\alpha_1 d\alpha_2 d\alpha_3 d\beta_1 d\beta_2 d\gamma_1 d\gamma_2 \delta\left(1 - \sum \alpha_j - \sum \beta_j - \sum \gamma_j\right) \int_{k_1} \int_{k_2} N_b^{(3)} / (\bar{D}_b^{(3)})^7. \quad (4.17)$$

Here the denominator is related to that of the u diagrams by the substitution $P_b \rightarrow -P_b$, and the equation corresponding to (4.9a) becomes

$$\Delta_b C = m^2 f_m - \tilde{r}^2 f_r - \alpha_1 \alpha_2 \alpha_3 s, \quad (4.18)$$

where f_m and f_r are given in (4.9b) and (4.9c). The numerator $N_b^{(3)}$ is similar to (4.2), with $u(P_b + r)$ and $\bar{u}(P_b - r)$ replaced by $v(P_b - r)$ and $\bar{v}(P_b + r)$, respectively. Following the same procedure as before, we find that

$$T_b'^{(3)} \approx (-ig)^6 i^7 (i\pi^2)^2 \left(\frac{1}{2\pi}\right)^8 \int d\alpha_1 d\alpha_2 d\alpha_3 d\beta_1 d\beta_2 d\gamma_1 d\gamma_2 \frac{1}{\bar{C}^2 (\bar{C}_{\Delta_b})} \delta\left(1 - \sum \alpha_j - \sum \beta_j - \sum \gamma_j\right) g^{\mu\rho} g^{\nu\lambda} t''_{\mu\nu\lambda\rho}, \quad (4.19)$$

where

$$\begin{aligned} g^{\mu\rho} g^{\nu\lambda} t''_{\mu\nu\lambda\rho} &= g^{\mu\rho} g^{\nu\lambda} \bar{u}(P_a + r) \gamma_\mu \gamma_\nu v(P_b - r) \bar{v}(P_b + r) \gamma_\lambda \gamma_\rho u(P_a - r) \\ &= 4s \delta_{\lambda_1 \lambda_3} \delta_{\lambda_2 \lambda_4} \delta_{\lambda_1 \lambda_2} + O(1). \end{aligned} \quad (4.20)$$

Except for the sign difference of the coefficient of s in the denominator, the evaluation of (4.19) is identical to that of (4.13a). We have

$$\begin{aligned} T_b^{(3)} &\approx -i \frac{g^2}{2!3!} \bar{g}^4 (\ln s - i\pi)^4 \\ &\quad \times \delta_{\lambda_1 \lambda_3} \delta_{\lambda_2 \lambda_4} \delta_{\lambda_1 \lambda_2}. \end{aligned}$$

The last four diagrams of Fig. 5(b) give identical contributions. Then

$$\begin{aligned} T_s^{(3)} &\approx 2T_b^{(3)} \\ &\approx -i 2 \frac{g^2}{2!3!} \bar{g}^4 (\ln s - i\pi)^4 \delta_{\lambda_1 \lambda_3} \delta_{\lambda_2 \lambda_4} \delta_{\lambda_1 \lambda_2}. \end{aligned} \quad (4.21)$$

The helicity structure is different from that of the corresponding fourth-order diagrams, but is similar to that of the fourth-order u diagrams. The calculation of the t diagrams, Fig. 6, follows the same procedure. Let us only mention the results: The diagrams of 6(a) behave at most like $\ln^3 s$, and 6(b) behave like $\ln s$. The additional planar t diagrams such as that shown in Fig. 7 go like

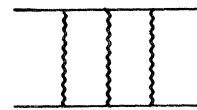


FIG. 7. Sixth-order t diagram with mesons all in the t channel.

1/s, up to powers of lns.

Let us remark that the behavior of the sixth-order diagrams we found above confirmed again the conjecture of Chang and Ma as mentioned in Sec. III.

For the nonplanar diagrams, the general analysis of Tiktopoulos²¹ shows that they cannot compete with their planar counterparts, and thus can be neglected unless cancellations occur among the planar ones, so that the maximum allowed powers of lns cannot be attained. In the present case, the leading terms do attain their maximum powers of lns. This result which we have shown for the fourth and sixth orders will be demonstrated for the higher orders in the next section. Hence nonplanar diagrams can be neglected. We have checked diagrams such as those shown in Fig. 8. The two diagrams go like lns and ln²s, respectively.

Similarly, diagrams which contain radiative corrections do not contribute to the leading logarithms. The diagrams with quartic vertices, for example Fig. 9, are asymptotically of order 1/s.

V. LEADING LOGARITHMS IN ALL ORDERS

We found in the last two sections that the *u*- and *s*-ladder diagrams dominate the fourth and sixth orders. In this section, we shall calculate these ladders as shown in Fig. 10, to all orders, assuming that they dominate. There are several reasons for assuming this: the trend suggested by the low-order diagrams as mentioned above, the similarity of the present cases and the *t*-channel ladders of the $(\varphi^3)_6$, and the Chang-Ma conjecture.

In order to simplify the calculation, we shall work with the forward spin-averaged amplitude only. Doing this, we lose the helicity information. The method used in this section follows closely that of Blaha, Ref. 24.

Consider the $2(n+1)$ -order *u* diagrams of the ladder form, as shown in Fig. 10(a). They all have the same denominator,

$$D_n = \prod_{j=1}^n \Delta_j^2 \prod_{i=1}^{n-1} [(k_i - k_{i+1})^2 - m^2] [(P_a - k_1)^2 - m^2] \times [(P_b - k_n)^2 - m^2], \quad (5.1a)$$

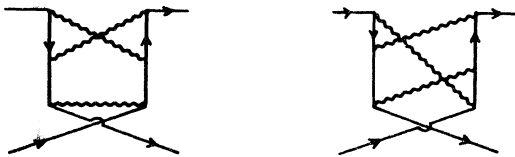


FIG. 8. Sixth-order nonplanar *s* diagrams.

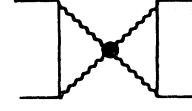


FIG. 9. Sixth-order diagram with a quartic vertex.

where

$$\Delta_j \equiv -(k_j^2 - m^2). \quad (5.1b)$$

The numerator of each individual diagram can be written as

$$\bar{u}(P_a) \Gamma_1(\not{k}_1 + m) \Gamma_2(\not{k}_2 + m) \cdots \Gamma_n(\not{k}_n + m) \Gamma_{n+1} u(P_b) \times \bar{u}(P_b) \Gamma_{n+1}(\not{k}_n + m) \Gamma_n \cdots \Gamma_2(\not{k}_1 + m) \Gamma_1 u(P_a), \quad (5.2a)$$

where

$$\Gamma_j = 1 \text{ or } -i\gamma_5$$

for scalar and pseudoscalar rungs, respectively. By spin averaging, the above expression becomes

$$\frac{1}{4} \text{Tr}[(\not{P}_a + m) \Gamma_1(\not{k}_1 + m) \Gamma_2(\not{k}_2 + m) \cdots (\not{k}_n + m) \times \Gamma_{n+1}(\not{P}_b + m) \Gamma_{n+1}(\not{k}_n + m) \cdots (\not{k}_1 + m) \Gamma_1] \quad (5.2b)$$

Let us denote the sum of all contributions such as (5.2b) by

$$N_n \equiv \frac{1}{4} \text{Tr}[(\not{P}_b + m) \not{P}_n]; \quad (5.3)$$

then

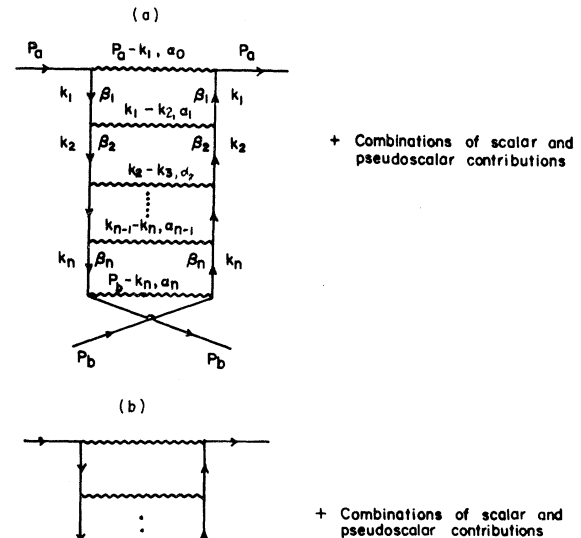


FIG. 10. *N*-loop ladder diagrams: (a) The *u* diagrams. Note that the momentum and Feynman parameter assignments have been displayed. (b) The *s* diagrams.

$$T_u^{(n+1)} \approx -(-ig)^{2(n+1)} i^{3n+1} \int_{k_1} \cdots \int_{k_n} \frac{N_n}{D_n}. \quad (5.4)$$

From a recursion formula, which we shall derive in Appendix B, P_n can be expanded in the form

$$2^{-(n+1)} P_n = A_n \not{p}_a + \sum_{j=1}^n B_n^j \not{k}_j, \quad (5.5)$$

where

$$\begin{aligned} A_n &= \prod_{j=1}^n \Delta_j, \\ B_n^j &= \left(\prod_{l=j+1}^n \Delta_l \right) \sum_{i=1}^j \sum_{1 \leq \lambda_1 < \lambda_2 < \cdots < \lambda_j = j} L_0^{\lambda_1} L_{\lambda_1}^{\lambda_2} \cdots L_{\lambda_{j-1}}^{\lambda_j}, \quad \lambda_j < n \\ B_n^n &= \sum_{i=1}^n \sum_{1 \leq \lambda_1 < \lambda_2 < \cdots < \lambda_i = n} L_0^{\lambda_1} L_{\lambda_1}^{\lambda_2} \cdots L_{\lambda_{i-1}}^{\lambda_i}, \\ L_i^j &= 2k_i \cdot k_j \prod_{l=i+1}^{j-1} \Delta_l, \quad j > i+1 \\ L_i^{i+1} &= 2k_i \cdot k_{i+1}. \end{aligned} \quad (5.6)$$

Substituting (5.5) into (5.3), we have

$$N_n = 2^{n+1} \left(A_n P_a \cdot P_b + \sum_{j=1}^n B_n^j P_b \cdot k_j \right). \quad (5.7)$$

To proceed further, we find it more convenient to parametrize the propagators in the exponential form in order to use the Mellin transformation. The following identities are needed:

$$\begin{aligned} (k^2 - m^2 + i\epsilon)^{-1} &= -i \int_0^\infty d\beta e^{i\beta(k^2 - m^2 + i\epsilon)}, \\ k_\mu k_\nu (k^2 - m^2 + i\epsilon)^{-2} &= \frac{+i}{2} \int_0^\infty d\beta \left[(2\beta)^{-1} \frac{\partial^2}{\partial a^\mu \partial a^\nu} - g_{\mu\nu} \right] e^{i\beta[(k+a)^2 - m^2 + i\epsilon]} \Big|_{a=0}. \end{aligned} \quad (5.8)$$

Let us first evaluate the contribution of the first term of Eq. (5.7). By leaving constant factors aside for the time being, we write

$$\begin{aligned} I_n(s) &= \int_{k_1} \cdots \int_{k_n} \frac{A_n}{D_n} \\ &= (-1)^n \int_{k_1} \cdots \int_{k_n} \left(\prod_{j=1}^n (k_j^2 - m^2 + i\epsilon) \right) \left\{ \prod_{i=1}^{n-1} [(k_i - k_{i+1})^2 - m^2 + i\epsilon] \right\} \\ &\quad \times [(P_a - k_1)^2 - m^2 + i\epsilon] [(P_b - k_n)^2 - m^2 + i\epsilon]^{-1} \\ &= (-1)^n (-i)^{2n+1} \int_0^\infty \prod_{l=0}^n d\alpha_l \prod_{j=1}^n d\beta_j \int_{k_1} \cdots \int_{k_n} \exp \left\{ \alpha_0 [(P_a - k_1)^2 - m^2 + i\epsilon] + \sum_{l=1}^{n-1} [(k_l - k_{l+1})^2 - m^2 + i\epsilon] \alpha_l \right. \\ &\quad \left. + [(P_b - k_n)^2 - m^2 + i\epsilon] \alpha_n + \sum_{j=1}^n (k_j^2 - m^2 + i\epsilon) \beta_j \right\}, \end{aligned} \quad (5.9)$$

where Eqs. (5.6) and (5.8) are used. The k_j integrations can be performed to give

$$\begin{aligned} I_n &= (-1)^n (-i)^{2n+1} (-i\pi^2)^n (2\pi)^{-4n} \\ &\quad \times \int_0^\infty \prod_{l=0}^n d\alpha_l \prod_{j=1}^n d\beta_j \frac{1}{C^2} e^{iD/C}. \end{aligned} \quad (5.10)$$

The homogeneous functions, D and C , can be obtained by means of the graphical cutting rules²⁵;

we list them below:

$$\begin{aligned} C &\equiv C_n^0 = d_{1,n} + (\alpha_0 + \beta_1) C_n^1 + \sum_{l=1}^{n-1} d_{1,l} \beta_{l+1} C_n^{l+1} \\ &= d_{0,n-1} + (\alpha_n + \beta_n) C_{n-1}^0 + \sum_{l=1}^{n-1} d_{l,n-1} \beta_l C_{l-1}^0, \end{aligned} \quad (5.11)$$

$$D = -s d_{0,n} - JC + i\epsilon,$$

where

$$d_{j,l} = \prod_{i=j}^l \alpha_i, \quad d_{j,j} = \alpha_j, \\ C_l^j = d_{j,l-1} + (\alpha_l + \beta_l) C_{l-1}^j + \sum_{i=j+1}^{l-1} d_{i,l-1} \beta_i C_{i-1}^j \quad (5.12) \\ = d_{j+1,l} + (\alpha_j + \beta_{j+1}) C_{l-1}^{j+1} + \sum_{i=j+1}^{l-1} d_{j+1,i} \beta_{i+1} C_i^{j+1}, \quad j < l$$

$$C_j^j = 1,$$

and

$$JC \equiv (m^2 - i\epsilon) \left\{ C \left[\sum_{l=1}^n (\alpha_l + \beta_l) - \alpha_n \right] \right. \\ \left. - 2d_{0,n} + \alpha_0^2 C_n^1 + \alpha_n^2 C_{n-1}^0 \right\}.$$

Take the Mellin transform of $I_n(s)$,

$$M_n(\omega) \equiv \int_0^\infty ds I_n(s) s^{-\omega-1} \\ = (4\pi)^{-2n} (-i)^{n+2} e^{i(\pi/2)\omega} \\ \times \Gamma(-\omega) \int_0^\infty \prod_{j=1}^n d\beta_j \prod_{i=0}^n d\alpha_i \alpha_i^\omega C^{-\omega-2} e^{-iJ}. \quad (5.13)$$

This expression has appeared in the discussion of high-energy behavior of the truss bridge diagrams of the $\varphi^3 + \varphi^4$ theory in four dimensions²⁶ and of the ladder diagrams in $(\varphi^3)_6$.¹² We shall refer to Ref. 26 for the details and give here the final result:

$$I_n(s) \sim (-i)^{n+2} (4\pi)^{-2n} \frac{1}{n!(n+1)!} \frac{1}{s} (\ln s)^{2n}. \quad (5.14)$$

This contributes to $T_u^{(n+1)}$ a term

$$-i g^2 \frac{\bar{g}^{2n}}{n!(n+1)!} \ln^{2n} s. \quad (5.15)$$

$$J_{n,l} \equiv \int_{k_1} \cdots \int_{k_n} \frac{1}{D_n} \left(\prod_{i=\lambda_l+1}^n \Delta_i \right) L_0^{\lambda_1} L_{\lambda_1}^{\lambda_2} \cdots L_{\lambda_{l-1}}^{\lambda_l} k_{\lambda_l} \cdot P_b \\ = 2^l (-1)^{n-l} g_{\mu_0 \nu_0} g_{\mu_1 \nu_1} \cdots g_{\mu_l \nu_l} P_a^{\mu_0} P_b^{\nu_l} \\ \times \int_{k_1} \cdots \int_{k_n} k_{\lambda_1}^{\nu_0} k_{\lambda_1}^{\mu_1} k_{\lambda_1}^{\nu_1} k_{\lambda_2}^{\mu_2} \cdots k_{\lambda_{l-1}}^{\nu_{l-1}} k_{\lambda_l}^{\mu_l} \\ \times \left((k_{\lambda_1}^2 - m^2 + i\epsilon) (k_{\lambda_2}^2 - m^2 + i\epsilon) \cdots (k_{\lambda_l}^2 - m^2 + i\epsilon) \right.$$

$$\left. \times \left[\prod_{e=1}^n (k_e^2 - m^2 + i\epsilon) \right] \left\{ \prod_{j=1}^{n-1} [(k_j - k_{j+1})^2 - m^2 + i\epsilon] \right\} [(P_a - k_1)^2 - m^2 + i\epsilon] [(P_b - k_n)^2 - m^2 + i\epsilon] \right\}^{-1}, \quad (5.16)$$

where $1 \leq \lambda_1 < \lambda_2 < \cdots < \lambda_l < n$. For $\lambda_l = n$, $\prod_{i=\lambda_l+1}^n \Delta_i$ is replaced by 1. Following Blaha,²⁴ we shall introduce n spurious momenta and replace the loop momenta which appear in the numerator by differentiations with respect to the spurious momenta.

Let us denote the spurious momenta by a_1, a_2, \dots, a_n . They enter or leave the vertices of a diagram as shown in Fig. 11. Using identities listed in (5.8), we write

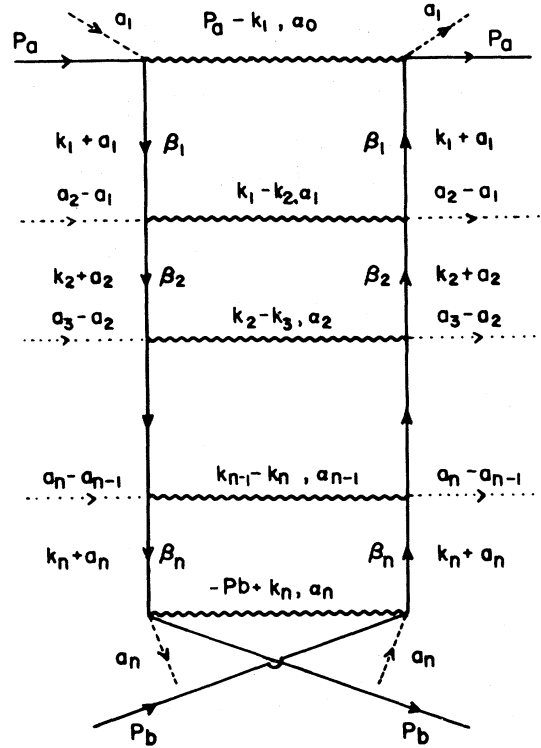


FIG. 11. N -loop ladder u diagrams with spurious momenta a_j and Feynman parameters α_j and β_j .

The evaluation of the contributions of the rest of the terms of (5.7) is very tedious. Fortunately, they are all nonleading. In the following, we give a brief description of this result. More details can be found in Appendix C.

A typical term of B_n^j which enters $T_u^{(n+1)}$ has the form

$$\begin{aligned}
J_{n,l} = & -i g_{\mu_0 \nu_0} g_{\mu_1 \nu_1} \cdots g_{\mu_l \nu_l} P_a^{\mu_0} P_b^{\nu_l} \\
& \times \int_0^\infty d\alpha_0 \cdots d\alpha_n d\beta_1 \cdots d\beta_n \left\{ \prod_{e=1}^l [g^{\nu_{e-1} \mu_e} - (2i\beta_{\lambda_e})^{-1} \mathfrak{D}_{\lambda_e}^{\nu_{e-1}} \mathfrak{D}_{\lambda_e}^{\mu_e}] \right\} \\
& \times \int_{k_1} \cdots \int_{k_n} \exp \left\{ i \sum_{j=1}^n [(k_j + a_j)^2 - m^2 + i\epsilon] \beta_j + i \sum_{j=1}^{n-1} [(k_j - k_{j+1})^2 - m^2 + i\epsilon] \alpha_j \right. \\
& \left. + i[(P_a - k_1)^2 - m^2 + i\epsilon] \alpha_0 + i[(P_b - k_n)^2 - m^2 + i\epsilon] \alpha_n \right\} \Big|_{a_1=a_2=\cdots=a_n=0},
\end{aligned}$$

where

$$\mathfrak{D}_{\lambda}^{\mu} \equiv \frac{\partial}{\partial a_{\lambda\mu}}. \quad (5.17)$$

Performing the loop-momentum integrations, we obtain

$$\begin{aligned}
J_{n,l} = & (-i)^{n+1} (4\pi)^{-2n} g_{\mu_0 \nu_0} g_{\mu_1 \nu_1} \cdots g_{\mu_l \nu_l} P_a^{\mu_0} P_b^{\nu_l} \\
& \times \int_0^\infty d\alpha_0 \cdots d\alpha_n d\beta_1 \cdots d\beta_n \left\{ \prod_{j=1}^l [g^{\nu_{j-1} \mu_j} - (2i\beta_{\lambda_j})^{-1} \mathfrak{D}_{\lambda_j}^{\nu_{j-1}} \mathfrak{D}_{\lambda_j}^{\mu_j}] \right\} \frac{1}{C^2} e^{iD(a)/C} \Big|_{a_1=\cdots=a_n=0},
\end{aligned} \quad (5.18)$$

where C is given in (5.11) and

$$D(a) = -d_{0,n} s + \sum_{l=1}^n [(P_a + a_l)^2 G_l + (P_b + a_l)^2 H_l] + \sum_{j,l=1}^n (a_j - a_l)^2 I_{jl} - (m^2 - i\epsilon) \left[C \left(\sum_{i=0}^n \alpha_i + \sum_{i=1}^n \beta_i \right) - 4d_{0,n} \right], \quad (5.19)$$

$$G_j = d_{0,j-1} \beta_j C_n^j,$$

$$H_j = d_{j,n} \beta_j C_{j-1}^0, \quad (5.20)$$

$$I_{jl} = d_{j,l-1} \beta_j \beta_l C_{j-1}^l C_n^l.$$

Clearly,

$$D(0) = D,$$

which is given in (5.11). Equation (5.19) can again be obtained by the graphic cutting rules²⁵ generalized to graphs containing $2n+6$ external lines.

The differentiations with respect to a_i in the integrand of (5.18) result in many terms. We keep only those, called the P terms, which can potentially contribute to an order of $\ln^{2n+2}s$. After factorizing powers of $d_{0,n} P_a \cdot P_b$, the remaining part of a P term must be nonvanishing for $\alpha_j = 0$, $j = 0, 1, 2, \dots, n$. For example, consider a term in the integrand of (5.18),

$$(-1)^e g_{\mu_0 \nu_0} g_{\mu_1 \nu_1} \cdots g_{\mu_e \nu_e} P_a^{\mu_0} P_b^{\nu_e} \left\{ \prod_{j=1}^e [(2i\beta_{\lambda_j})^{-1} \mathfrak{D}_{\lambda_j}^{\nu_{j-1}} \mathfrak{D}_{\lambda_j}^{\mu_j}] \right\} \frac{1}{C^2} e^{iD(a)/C} \Big|_{a_1=\cdots=a_n=0}. \quad (5.21)$$

We shall demonstrate in Appendix C that the P terms of (5.21) are of the form

$$(-1)^e \frac{1}{C^2} e^{iD/C} (P_a \cdot P_b) \left(\prod_{j=1}^e \Sigma_{\lambda_j} \right) \sum_{j=0}^{e-1} \frac{i^{e-j}}{C^{2e-j}} (-1)^j S_e^{(j)} (2d_{0,n} P_a \cdot P_b)^{e-j}, \quad (5.22)$$

where $S_e^{(j)}$ is the Stirling number of the second kind²⁷ and

$$\Sigma_{\lambda} \equiv C_{\lambda-1}^0 \beta_{\lambda} C_n^{\lambda}. \quad (5.23)$$

Let us change the variables

$$\begin{aligned}
\alpha_j &= \rho \bar{\alpha}_j, \quad j = 0, 1, \dots, n \\
\beta_l &= \rho \bar{\beta}_l, \quad l = 1, 2, \dots, n
\end{aligned} \quad (5.24)$$

$$\sum_{j=0}^n \bar{\alpha}_j + \sum_{l=1}^n \bar{\beta}_l = 1.$$

Recall that D , C , $C_{\lambda-1}^0$, C_n^λ , and $d_{0,n}$ are respectively homogeneous functions of degree $n+1$, n , $\lambda-1$, $n-\lambda$, and $n+1$. Equation (5.22) becomes

$$(-1)^e \rho^{-2n} \frac{1}{C^2} e^{i\rho \bar{D}/\bar{C}} (P_a \cdot P_b) \left(\prod_{j'=1}^e \bar{\Sigma}_{\lambda_{j'}} \right) \sum_{j=0}^{e-1} (-1)^j \rho^{e-j} \frac{i^{e-j}}{C^{2e-j}} S_e^{(j)} (2\bar{d}_{0,n} P_a \cdot P_b)^{e-j}, \quad (5.25)$$

where \bar{D} , \bar{C} , etc. are obtained from D , C , etc. by replacing α_j and β_j by $\bar{\alpha}_j$ and $\bar{\beta}_j$. Substituting (5.25) into (5.18) and performing the ρ integration, we see that (5.25) is

$$i(-1)^e \frac{(P_a \cdot P_b)}{C^2} \left(\prod_{j'=1}^e \bar{\Sigma}_{\lambda_{j'}} \right) \sum_{j=0}^{e-1} \frac{(-1)^e}{C^{2e-j}} (e-j)! S_e^{(j)} \left(\frac{\bar{C}}{\bar{D}} \right)^{e-j+1} (2\bar{d}_{0,n} P_a \cdot P_b)^{e-j} \\ \simeq i(-1)^e \frac{(P_a \cdot P_b)}{C\bar{D}} \left(\prod_{j'=1}^e \frac{\bar{\Sigma}_{\lambda_{j'}}}{\bar{C}} \right) \sum_{j=0}^{e-1} (-1)^j (e-j)! S_e^{(j)}, \quad (5.26)$$

where we have used

$$\int_0^\infty d\rho \rho^\lambda e^{i\rho(\bar{D}/\bar{C})} = i^{\lambda+1} \lambda! \left(\frac{\bar{C}}{\bar{D}} \right)^{\lambda+1}, \quad (5.27)$$

and have made the approximation

$$2d_{0,n} P_a \cdot P_b / D \simeq -1.$$

We can prove from probability theory that²⁸

$$\sum_{j=0}^{e-1} (-1)^j (e-j)! S_e^{(j)} = 1. \quad (5.28)$$

Equation (5.26) becomes

$$i(-1)^e \frac{1}{C\bar{D}} \prod_{j=1}^e \left(\frac{\bar{\Sigma}_{\lambda_j}}{\bar{C}} \right). \quad (5.29)$$

Now it is easy to see that

$$J_{n,i} = (-i)^n (4\pi)^{-2n} \int_0^1 d\bar{\alpha}_0 \cdots d\bar{\alpha}_n d\bar{\beta}_1 \cdots d\bar{\beta}_n \\ \times \delta \left(1 - \sum \bar{\alpha}_e - \sum \bar{\beta}_e \right) \\ \times \frac{(P_a \cdot P_b)}{C\bar{D}} \prod_{j=1}^e \left(1 - \frac{\bar{\Sigma}_{\lambda_j}}{\bar{C}} \right). \quad (5.30)$$

We shall show in Appendix C that

$$\bar{C} - \bar{\Sigma}_\lambda = (\bar{\alpha}_{\lambda-1} + \bar{\alpha}_\lambda) \bar{C}_{\lambda-1}^0 \bar{C}_n^\lambda \\ + \text{terms quadratic in } \bar{\alpha}'\text{'s}. \quad (5.31)$$

This clearly shows that $J_{n,i}$ does not give rise to a $\ln^{2n}s$ term.

Since the contributions of B_n^j , $i=1, 2, \dots, n$ are all of the form of $J_{n,i}$, they are all nonleading. Consequently, the leading term of $T_u^{(n+1)}$ is given by that of $I_n(s)$:

$$T_u^{(n+1)} = -ig^2 \frac{1}{n! (n+1)!} (\bar{g}^2 \ln^2 s)^n. \quad (5.32)$$

In the special cases $n=0, 1$, and 2 , Eq. (5.32) agrees with the spin-averaged amplitudes of the second, fourth, and sixth orders. [See Eqs. (3.26), (3.17), and (4.16).]

The high-energy behavior of the s diagrams can be obtained in exactly the same way. We shall mention quickly where they differ from the u diagrams. The numerator of an s diagram is similar to that of the corresponding u diagram, i.e., Eq. (5.2a), except that the factor $u(P_b) \bar{u}(P_b)$ is replaced by $v(P_b) \bar{v}(P_b)$. Consequently, the sum of all the numerators is given by (5.3) if $P_b + m$ is replaced by $P_b - m$. However, this will not change the final result; both (5.5) and (5.7) are still valid. For the denominator, we need only to replace the factor $[(P_b + k_n)^2 - m^2]$ in (5.1a) by $[(P_b + k_n)^2 - m^2]$. This results in changing s into $-s$ in D and $D(0)$ given by Eqs. (5.11) and (5.19). Except for these straightforward modifications, all the other expressions remain valid. Following the same procedure, we again find that the $A_n P_a \cdot P_b$ term [see Eq. (5.5)] gives the leading term, and finally we arrive at the result

$$T_s^{n+1} \approx -ig^2 \frac{1}{n! (n+1)!} [\bar{g}^2 (\ln s - i\pi)^2]^n. \quad (5.33)$$

Now we can sum to all orders the leading logarithms of the two classes of diagrams:

$$T_u = \sum_{n=0}^{\infty} T_u^{(n+1)} \\ = -ig^2 \sum_{n=0}^{\infty} \frac{1}{n! (n+1)!} (\bar{g}^2 \ln^2 s)^n \\ = -ig^2 \frac{I_1(2\bar{g} \ln s)}{\bar{g} \ln s} \\ \approx -\frac{ig^2}{\sqrt{4\pi}} \frac{s^{2\bar{g}}}{(\bar{g} \ln s)^{3/2}} \quad (5.34)$$

and

$$T_s = -ig^2 \frac{I_1(2\bar{g}(\ln s - i\pi))}{\bar{g} \ln s} \\ \approx -\frac{ig^2}{\sqrt{4\pi}} e^{-i2\pi\bar{g}} \frac{s^{2\bar{g}}}{(\bar{g} \ln s)^{3/2}}. \quad (5.35)$$

For the s model, the amplitude is

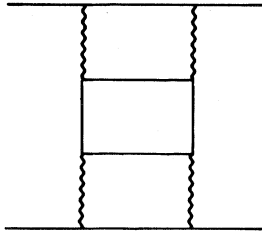


FIG. 12. Eighth-order diagram containing a meson-meson scattering subdiagram.

$$T = T_s + T_u$$

$$\approx -\frac{ig^2}{\sqrt{4\pi}} (1 + e^{-i2\pi\bar{g}}) \frac{s^{2\bar{g}}}{(\bar{g} \ln s)^{3/2}}. \quad (5.36)$$

This is a fixed cut and is similar to the results of $(\varphi^3)_6$ and the truss bridge diagrams of $\varphi^3 + \varphi^4$ theory in four dimensions, except that the signature is opposite.

In the σ model the fermion-fermion and fermion-antifermion scattering amplitudes are given respectively by T_u and T_s , Eqs. (5.34) and (5.35). Similar results hold in the Y model if we replace g and \bar{g} by $g/\sqrt{2}$ and $\bar{g}/\sqrt{2}$ in the two equations, since only the pseudoscalar is exchanged here. If a scalar meson replaces the pseudoscalar in the Y model, we obtain the same result. The above result of the fermion-antifermion scattering in the Y model agrees with that of Swift and Lee,²⁹ obtained by means of the Bethe-Salpeter equation.

To conclude this section, let us mention that a new class of diagrams which contain meson-meson scattering as subdiagrams appear in eighth or higher orders. An example of such diagrams in eighth order is shown in Fig. 12. The meson-meson scattering subdiagrams require renormalization. We have examined this diagram in some detail and have found that it is nonleading.

VI. CONCLUSION

We have studied the fermion-fermion and fermion-antifermion scatterings in a class of field theories containing fermions and spinless mesons. In the high-energy limit, the diagrams with fermions exchanged in the t channel dominate in all orders of the perturbation expansion. They are ladder diagrams with scalars or pseudoscalars as rungs and fermions running along the sides. This result agrees with the conjecture made by Chang and Ma in a QED calculation. It is reminiscent of the basic rule of Reggeology that an amplitude is dominated by the highest J -plane trajectory allowed in the t channel, although there is no connection whatsoever between the masses

and spins of particles in a field theory. A similar class of diagrams have in fact been used by Drell, Levy, and Yan³⁰ some time ago as the dominant diagrams in the deep-inelastic electron-proton scattering in a P_1 cutoff Yukawa theory.

The results of Secs. III and IV show that the dominant helicity amplitudes are different in the fourth and sixth orders. We have not investigated whether this pattern of change will be repeated regularly in higher orders, nor have we addressed ourselves to the question of summing the helicity amplitudes (perhaps of alternating orders).

Despite the fact that the supersymmetry alters some aspects of the renormalization, it has the basic features of the high-energy behavior of the Y and σ models. The high-energy amplitude is a $\ln^2 s$ series and lacks P_1 damping. This is in contrast with the SBNGT where a Reggeized amplitude corresponding to the exchange of vector-meson Regge trajectory results after cancellations among diagrams. Based on our results, it is interesting to compare the high-energy behavior of a supersymmetric theory and an SBNGT. The similarity is that they have high symmetries which dictate that in each theory the coupling constant is degenerate. There are important differences. In the SBNGT, the vector meson, since it is the highest-spin particle, crucially determines the leading logarithms of the amplitude. Therefore, the vector-meson self-coupling, e.g., the triple vertices, can play an important role. (They indeed do.) However, in the supersymmetric theory, the spinless mesons seem to play only a supporting role; they provide momentum transfer for the fermions so that the latter can run along the t channel and then emerge again in the final state, or be annihilated. Hence, the meson-meson coupling does not have any effect in the determination of the leading terms.

Despite its passiveness as described above, the supersymmetry may play a more active role in the fermion-meson and meson-meson scatterings. The following areas are especially pertinent: (a) the relationship among the fermion-fermion, fermion-meson, and meson-meson amplitudes, (b) the possibility of cancellation of large-transverse-momentum contributions in the fermion-meson and meson-meson channels in which the mesonic self-interactions may be more important. These interesting questions, which are beyond the scope of the present paper, will be addressed in a future work.

As a final remark, in an ordinary SBNGT, the asymptotic freedom could in general be destroyed.³¹ However, a theory which is both supersymmetric and non-Abelian gauge invariant is an exception.³² Our calculation may be useful

in the study of the high-energy behavior of this interesting theory.

ACKNOWLEDGMENTS

This work was initiated when two of the authors (T. F. W. and B. L. Y.) visited the Aspen Summer Institute in 1975. We thank Professor L. Durand for the hospitality extended to us. Discussions with Paul Langacker and Terry Hagiwara (both collaborated with us in the early phase of this work), and with David Harrington, Tai-Tsun Wu, John Galayda, and B. C. Carlson are gratefully acknowledged. We would also like to thank Professor S. Gasiorowicz for discussions and for his lecture notes on supersymmetry and Majorana fields.

APPENDIX A

In this appendix, we collect several results which are relevant to our calculation. A Majorana spinor ψ is defined by

$$\psi = \psi^c \equiv (\bar{\psi}c)^T, \quad (A1)$$

where²² $c = i\gamma_0\gamma_2$ is the charge conjugation matrix. Properties of ψ can be read off directly from those of a Dirac spinor χ , if ψ is identified with $(1/\sqrt{2})[\chi + (\bar{\chi}c)^T]$.³³ We note that there is no fermion number associated with the quanta of a Majorana spinor field. Because of (A1), ψ and $\bar{\psi}$ are not independent fields:

$$\bar{\psi}_\alpha = \psi_\beta c_{\beta\alpha}^{-1}. \quad (A2)$$

This is the reason why a factor $\frac{1}{2}$ is needed in front of the kinetic energy and mass terms of \mathcal{L}_s , Eq. (2.1). Bearing this in mind, we can derive the Feynman rules as given in Fig. 1.

Next we list formulas of spinor wave functions needed to calculate the helicity amplitudes of Secs. III and IV. The u and v spinors are related by

$$\begin{aligned} v_\alpha(P, s) &= \bar{u}_\beta(P, s) c_{\beta\alpha}, \\ \bar{v}_\alpha(P, s) &= -c_{\alpha\beta}^{-1} u_\beta(P, s), \\ u_\alpha(P, s) &= \bar{v}_\beta(P, s) c_{\beta\alpha}, \\ \bar{u}_\alpha(P, s) &= -c_{\alpha\beta}^{-1} v_\beta(P, s). \end{aligned} \quad (A3)$$

The following relations follow straightforwardly:

$$\begin{aligned} \bar{v}(P_1, s_1) \Gamma v(P_2, s_2) &= -\bar{u}(P_2, s_2) c \Gamma^T c^{-1} u(P_1, s_1), \\ \bar{u}(P_1, s_1) \Gamma v(P_2, s_2) &= -\bar{u}(P_2, s_2) c \Gamma^T c^{-1} v(P_1, s_1), \\ \bar{v}(P_1, s_1) \Gamma u(P_2, s_2) &= -\bar{v}(P_2, s_2) c \Gamma^T c^{-1} u(P_1, s_1), \end{aligned} \quad (A4)$$

where

$$c\gamma_\mu c^{-1} = -\gamma_\mu^T.$$

The relations in (A4) are needed to verify our

statement in the third paragraph of Sec. III concerning the use of u and v spinors.

The explicit forms of the spinor wave functions,²² with helicity $\pm\frac{1}{2}$, are

$$\begin{aligned} u(P, s) &= (E+m)^{1/2} \begin{pmatrix} \chi_s \\ \frac{\vec{\sigma} \cdot \vec{p}}{E+m} \chi_s \end{pmatrix}, \\ v(P, s) &= (E+m)^{1/2} \begin{pmatrix} \frac{\vec{\sigma} \cdot \vec{p}}{E+m} \xi_s \\ \xi_s \end{pmatrix}, \end{aligned} \quad (A5)$$

where χ_s is a nonrelativistic spinor wave function satisfying

$$\vec{\sigma} \cdot \frac{\vec{p}}{|\vec{p}|} \chi_s = s \chi_s, \quad s = \pm 1 \quad (A6)$$

and

$$\xi_s \equiv -i\sigma_2(\chi_s^t)^T. \quad (A7)$$

If we choose the reaction plane to coincide with the zx plane so that $r = (0, r, 0, 0)$, then in the limit $r/E \rightarrow 0$

$$\begin{aligned} \chi_\pm^{(1)} &\simeq \eta_\pm \mp \frac{r}{\sqrt{s}} \eta_\mp, & \chi_\pm^{(3)} &\simeq \eta_\pm \pm \frac{r}{\sqrt{s}} \eta_\mp, \\ \chi_\pm^{(2)} &\simeq \eta_\mp \pm \frac{r}{\sqrt{s}} \eta_\pm, & \chi_\pm^{(4)} &\simeq \eta_\mp \mp \frac{r}{\sqrt{s}} \eta_\pm, \\ \xi_\pm^{(2)} &= \mp \chi_\mp^{(2)}, & \xi_\pm^{(4)} &= \mp \chi_\mp^{(4)}, \end{aligned} \quad (A8)$$

and

$$\eta_+ = \begin{pmatrix} 1 \\ 0 \end{pmatrix}, \quad \eta_- = \begin{pmatrix} 0 \\ 1 \end{pmatrix},$$

where $\chi_\pm^{(1)}$, etc. apply to particle 1, etc. Equations (A5) and (A8) enable us to calculate the helicity amplitudes of Secs. III and IV.

APPENDIX B

To prove (5.5) and (5.6), let us fix our attention on the last fermion propagator carrying the momentum k_n on each side of the ladder [see Fig. 11(a)]. We can divide all the diagrams with $n+1$ rungs into two groups. One group has the last rungs of the ladders (with momentum $P_b - k_n$) as scalars, the other as pseudoscalars. The numerator of each group is given by P_{n-1} . Then

$$\begin{aligned} \frac{1}{2} P_n &= \frac{1}{\sqrt{2}} (\not{k}_n + m) P_{n-1} (\not{k}_n + m) \frac{1}{\sqrt{2}} \\ &\quad - \frac{1}{\sqrt{2}} \gamma_5 (\not{k}_n + m) P_{n-1} (\not{k}_n + m) \gamma_5 \frac{1}{\sqrt{2}}. \end{aligned} \quad (B1)$$

We give the results of two simple cases:

$$\frac{1}{2} P_0 = \not{P}_a \quad (B2a)$$

for the Born diagrams and

$$\begin{aligned} (\tfrac{1}{2})^2 P_1 &= \tfrac{1}{2}(\not{k}_1 + m) \left(\frac{P_0}{2} \right) (\not{k}_1 + m) \\ &\quad - \tfrac{1}{2} \gamma_5 (\not{k}_1 + m) \frac{P_0}{2} (\not{k}_1 + m) \gamma_5 \\ &= -(k^2 - m^2) \not{P}_a + 2(P_a \cdot k_1) \not{k}_1 \end{aligned} \quad (\text{B2b})$$

for the box diagrams. Let us now write

$$(\tfrac{1}{2})^{n+1} P_n = A_n \not{P}_a + \sum_{j=1}^n B_n^j \not{k}_j. \quad (\text{B3})$$

Substituting it into (B1), we have

$$\begin{aligned} (\tfrac{1}{2})^{n+1} P_n &= A_{n-1} \Delta_n \not{P}_n + \sum_{j=1}^{n-1} \Delta_n B_{n-1}^j \not{k}_j \\ &\quad + \left[L_0^n + \sum_{j=1}^{n-1} 2(k_n \cdot k_j) B_{n-1}^j \right] \not{k}_n, \end{aligned} \quad (\text{B4})$$

where Δ_n and L_0^n are defined in (5.1b) and (5.6). The solutions of (B4) with the boundary conditions (B2b) are just (5.6).

These results hold also for the σ model as long as a degenerate mass for the scalar and pseudo-scalar is used in the perturbation expansion. In the Y model there is no scalar; the effect is that the terms which contribute to the leading logarithm are reduced by a factor $(\tfrac{1}{2})^n$ for the n th-order ladders. This amounts to replacing the coupling constant g in the s or σ model by $(1/\sqrt{2})g$.

APPENDIX C

In this appendix we shall present some details on our assertion that the terms proportional to B_n^j in (5.7) do not contribute to the leading logarithms. Our main task is to prove (5.22) and (5.32). Although the method used here is close to that of Ref. 24, there are enough differences, especially in the latter part of our proof, that a discussion of some of the crucial steps is warranted.

Let us define

$$\begin{aligned} (j)_\mu &\equiv d_{0,j-1} C_n^j P_{a\mu} + d_{j,n} C_{j-1}^0 P_{b\mu}, \\ (jj) &\equiv \frac{1}{\beta_j} [\alpha_{j-1} C_n^j (C_{j-1}^0 - \alpha_{j-1} C_{j-2}^0) \\ &\quad + \alpha_j C_{j-1}^0 (C_n^j - \alpha_j C_n^{j+1})], \\ (j_l) &= -d_{j,l-1} C_{j-1}^0 C_n^l, \quad j < l \end{aligned} \quad (\text{C1})$$

where $d_{j,l}$ and C_l^j are given in (5.11) and (5.12). Keeping terms with lowest power in α_j 's and highest power in $P_a \cdot P_b$, we have for $j_1 < j_2$

$$\begin{aligned} (j_1 \cdot j_2) &\equiv (j_1)_\mu (j_2)^\mu \simeq d_{j_1, j_2-1}^{-1} C_n^{j_1} C_{j_2-1}^0 [d_{0,n} (P_a \cdot P_b)], \\ (j_1 \cdot j_1) &\equiv (j_1)_\mu (j_1)^\mu \simeq C_{j_1-1}^0 C_n^{j_1} [2d_{0,n} (P_a \cdot P_b)], \\ (P_a \cdot j) &\equiv P_a^\mu (j)_\mu \simeq d_{j,n} C_{j-1}^0 (P_a \cdot P_b), \\ (P_b \cdot j) &\equiv P_b^\mu (j)_\mu \simeq d_{0,j-1} C_n^j (P_a \cdot P_b), \\ (P_a \cdot j_1)(P_b \cdot j_2) &\simeq d_{j_1, j_2-1} C_{j_1-1}^0 C_n^{j_2} [d_{0,n} (P_a \cdot P_b)^2], \\ (P_a \cdot j_2)(P_b \cdot j_1) &\simeq d_{j_1, j_2-1}^{-1} C_{j_2-1}^0 C_n^{j_1} [d_{0,n} (P_a \cdot P_b)^2], \\ (P_a \cdot j_1)(P_b \cdot j_1) &\simeq C_{j_1-1}^0 C_n^{j_1} [d_{0,n} (P_a \cdot P_b)^2]. \end{aligned} \quad (\text{C2})$$

We note the following formulas:

$$\begin{aligned} \frac{1}{\beta_l} \frac{i}{C} \frac{\partial D(a)}{\partial a_l^\mu} \Big|_{a_j=0} &= \frac{2i}{C} (l)_\mu, \\ \frac{1}{\beta_l \beta_j} \frac{i}{C} \frac{\partial^2 D(a)}{\partial a_l^\mu \partial a_j^\nu} \Big|_{a_i=0} &= \frac{2i}{C} (jl)_{g\mu\nu}. \end{aligned} \quad (\text{C3})$$

Consider now the integrand of (5.18)

$$\frac{1}{C^2} \prod_{j=1}^l [g^{\mu_j - 1} \nu_j - (2i\beta_{\lambda_j})^{-1} \mathfrak{D}_{\lambda_j}^{\mu_j - 1} \mathfrak{D}_{\lambda_j}^{\nu_j}] e^{iD(a)/C} \Big|_{a=0}, \quad (\text{C4})$$

where \mathfrak{D}_λ^ν is defined in (5.17). To get a feeling about the terms involved in this expression, we consider in detail a simple case,

$$(\beta_{\lambda_1} \beta_{\lambda_2})^{-1} \mathfrak{D}_{\lambda_1}^{\mu_1} \mathfrak{D}_{\lambda_2}^{\nu_2} e^{iD(a)/C} \Big|_{a=0} = \left[\frac{2i}{C} g^{\mu\nu} (\lambda_1 \lambda_2) + \left(\frac{2i}{C} \right)^2 (\lambda_1)^\mu (\lambda_2)^\nu \right] e^{iD/C}, \quad (\text{C5})$$

$$\begin{aligned} \prod_{j=1}^4 (\beta_{\lambda_j})^{-1} \mathfrak{D}_{\lambda_j}^{\mu_j} e^{iD(a)/C} \Big|_{a=0} &= e^{iD/C} \left\{ \left(\frac{2i}{C} \right)^2 [g^{\mu_1 \mu_2} g^{\mu_3 \mu_4} (\lambda_1 \lambda_2) (\lambda_3 \lambda_4) + g^{\mu_1 \mu_3} g^{\mu_2 \mu_4} (\lambda_1 \lambda_3) (\lambda_2 \lambda_4) + g^{\mu_1 \mu_4} g^{\mu_2 \mu_3} (\lambda_1 \lambda_4) (\lambda_2 \lambda_3)] \right. \\ &\quad + \left(\frac{2i}{C} \right)^3 [g^{\mu_1 \mu_2} (\lambda_1 \lambda_2) (\lambda_3)^\mu (\lambda_4)^\mu + g^{\mu_1 \mu_3} (\lambda_1 \lambda_3) (\lambda_2)^\mu (\lambda_4)^\mu \\ &\quad + g^{\mu_1 \mu_4} (\lambda_1 \lambda_4) (\lambda_2)^\mu (\lambda_3)^\mu + g^{\mu_2 \mu_3} (\lambda_2 \lambda_3) (\lambda_1)^\mu (\lambda_4)^\mu \\ &\quad + g^{\mu_2 \mu_4} (\lambda_2 \lambda_4) (\lambda_1)^\mu (\lambda_3)^\mu + g^{\mu_3 \mu_4} (\lambda_3 \lambda_4) (\lambda_1)^\mu (\lambda_2)^\mu] \\ &\quad \left. + \left(\frac{2i}{C} \right)^4 (\lambda_1)^\mu (\lambda_2)^\mu (\lambda_3)^\mu (\lambda_4)^\mu \right\}. \end{aligned} \quad (\text{C6})$$

If we relate $g_{\mu_1\mu_2}g_{\mu_3\mu_4}(\lambda_1\lambda_2)(\lambda_3\lambda_4)$ with the permutation (12)(34), $g^{\mu_1\mu_2}(\lambda_1\lambda_2)(\lambda_3)(\lambda_4)^{\mu_4}$ with (12)(3)(4), and $(\lambda_1)^{\mu_1}(\lambda_2)^{\mu_2}(\lambda_3)^{\mu_3}(\lambda_4)^{\mu_4}$ with (1)(2)(3)(4), the coefficients of $(2i/C)^n$, $n = 2, 3, 4$ can be identified with the collections of elements $\{2^2\}$, $\{2\ 1^2\}$, and $\{1^4\}$ of the symmetry group of four objects. Using this result we can write

$$\prod_{j=0}^{2l} \beta_{\lambda_j}^{-1} \mathfrak{D}_{\lambda_j}^{\mu_j} e^{iD(a)/C} \Big|_{a_i=0} = \sum_{j=0}^l \left(\frac{2i}{C}\right)^{l+j} \{2^l - j\ 1^{2j}\}. \quad (C7)$$

To illustrate the essential points, we consider a special case of (5.18) and show that it *does not* contribute to the leading logarithm:

$$I_{\lambda_1\lambda_2} = \int_0^\infty d\alpha_0 \cdots d\alpha_n d\beta_1 \cdots d\beta_n g_{\mu_0\nu_0} g_{\mu_1\nu_1} g_{\mu_2\nu_2} P_a^{\mu_0} P_b^{\nu_2} \\ \times [g^{\nu_0\mu_1} - (2i\beta_{\lambda_1})^{-1} \mathfrak{D}_{\lambda_1}^{\nu_0} \mathfrak{D}_{\lambda_1}^{\mu_1}] [g^{\nu_1\mu_2} - (2i\beta_{\lambda_2})^{-1} \mathfrak{D}_{\lambda_2}^{\nu_1} \mathfrak{D}_{\lambda_2}^{\mu_2}] \frac{1}{C^2} e^{iD(a)/C} \Big|_{a=0}, \quad \lambda_1 < \lambda_2. \quad (C8)$$

The integrand is

$$\frac{1}{C^2} g_{\mu_0\nu_0} g_{\mu_1\nu_1} g_{\mu_2\nu_2} P_a^{\mu_0} P_b^{\nu_2} [g^{\nu_0\mu_1} g^{\nu_1\mu_2} - (2i\beta_{\lambda_1})^{-1} g^{\nu_1\mu_2} \mathfrak{D}_{\lambda_1}^{\nu_0} \mathfrak{D}_{\lambda_1}^{\mu_1} - (2i\beta_{\lambda_2})^{-1} g^{\nu_0\mu_1} \mathfrak{D}_{\lambda_2}^{\nu_1} \mathfrak{D}_{\lambda_2}^{\mu_2} \\ + (2i\beta_{\lambda_1})^{-1} (2i\beta_{\lambda_2})^{-1} \mathfrak{D}_{\lambda_1}^{\nu_0} \mathfrak{D}_{\lambda_1}^{\mu_1} \mathfrak{D}_{\lambda_2}^{\nu_1} \mathfrak{D}_{\lambda_2}^{\mu_2}] e^{iD(a)/C} \Big|_{a=0} \\ = \frac{1}{C^2} e^{iD/C} \left\{ P_a \cdot P_b - (2i\beta_{\lambda_2}) \left(\frac{1}{2i}\right)^2 \left[\frac{2i}{C} (\lambda_2 \lambda_2) (P_a \cdot P_b) + \left(\frac{2i}{C}\right)^2 (P_a \cdot \lambda_2) (P_b \cdot \lambda_2) \right] \right. \\ - (2i\beta_{\lambda_1}) \left(\frac{1}{2i}\right)^2 \left[\frac{2i}{C} (\lambda_1 \lambda_1) (P_a \cdot P_b) + \left(\frac{2i}{C}\right)^2 (P_a \cdot \lambda_1) (P_b \cdot \lambda_1) \right] \\ + (2i\beta_{\lambda_1}) (2i\beta_{\lambda_2}) \left(\frac{1}{2i}\right)^4 \left[\left(\frac{2i}{C}\right)^2 (\lambda_1 \lambda_1) (\lambda_2 \lambda_2) + 5(\lambda_1 \lambda_2)^2 (P_a \cdot P_b) \right. \\ \left. + \left(\frac{2i}{C}\right)^3 ((\lambda_1 \lambda_1) (P_a \cdot \lambda_2) (P_b \cdot \lambda_2) + 6(\lambda_1 \lambda_2) (P_a \cdot \lambda_1) (P_b \cdot \lambda_2) \right. \\ \left. + (\lambda_1 \lambda_2) (\lambda_1 \cdot \lambda_2) P_a \cdot P_b + (\lambda_2 \lambda_2) (P_a \cdot \lambda_1) (P_b \cdot \lambda_1)) \right. \\ \left. + \left(\frac{2i}{C}\right)^4 (\lambda_1 \cdot \lambda_2) (P_a \cdot \lambda_1) (P_b \cdot \lambda_2) \right] \Big\}. \quad (C9)$$

From (B1) and (B2), we note that all the terms in this expression can be put in the form

$$f(\alpha, \beta) \frac{P_a \cdot P_b}{C^2} e^{iD/C} (d_{0,n} P_a \cdot P_b)^l, \quad l = 0, 1, 2.$$

The leading contributions arise from the part of $f(\alpha, \beta)$ which does not vanish for $\alpha_j = 0$, $j = 0, 1, \dots, n$. By means of this criterion, we can write (C9) as

$$\frac{1}{C^2} e^{iD/C} \left\{ P_a \cdot P_b - \frac{2i\beta_{\lambda_1}}{C^2} (P_a \cdot \lambda_2) (P_b \cdot \lambda_2) - \frac{2i\beta_{\lambda_2}}{C^2} (P_a \cdot \lambda_1) (P_b \cdot \lambda_1) \right. \\ \left. + (2i\beta_{\lambda_1}) (2i\beta_{\lambda_2}) \left(\frac{1}{2i}\right)^4 \left[\left(\frac{2i}{C}\right)^3 (\lambda_1 \lambda_2) (\lambda_1 \cdot \lambda_2) P_a \cdot P_b + \left(\frac{2i}{C}\right)^4 (\lambda_1 \cdot \lambda_2) (P_a \cdot \lambda_1) (P_b \cdot \lambda_2) \right] \right\} \\ \simeq \frac{1}{C^2} e^{iD/C} (P_a \cdot P_b) \left[1 - \frac{i\beta_{\lambda_1}}{C^2} C_{\lambda_1-1}^0 C_n^{\lambda_1} (2P_a \cdot P_b d_{0,n}) - \frac{i\beta_{\lambda_2}}{C^2} C_{\lambda_2-1}^0 C_n^{\lambda_2} (2P_a \cdot P_b d_{0,n}) \right. \\ - i \frac{\beta_{\lambda_1} \beta_{\lambda_2}}{C^3} C_{\lambda_1-1}^0 C_n^{\lambda_1} C_{\lambda_2-1}^0 C_n^{\lambda_2} (2P_a \cdot P_b d_{0,n}) \\ \left. - \frac{\beta_{\lambda_1} \beta_{\lambda_2}}{C^4} C_{\lambda_1-1}^0 C_n^{\lambda_1} C_{\lambda_2-1}^0 C_n^{\lambda_2} (2P_a \cdot P_b d_{0,n})^2 \right]. \quad (C10)$$

Substituting this into (C8), we arrive at the result

$$\begin{aligned}
I_{\lambda_1 \lambda_2} &= i(P_a \cdot P_b) \int_0^1 d\bar{\alpha}_0 d\bar{\alpha}_1 \cdots d\bar{\alpha}_n d\bar{\beta}_1 \cdots d\bar{\beta}_n \delta \left(1 - \sum \bar{\alpha}_j - \sum \bar{\beta}_j \right) \\
&\quad \times \frac{1}{CD} \left\{ 1 + \frac{\bar{\beta}_{\lambda_2} \bar{C}_{\lambda_2-1}^0 \bar{C}_n^{\lambda_2}}{\bar{C}} \frac{2P_a \cdot P_b \bar{d}_{0,n}}{\bar{D}} + \frac{\bar{\beta}_{\lambda_1} \bar{C}_{\lambda_1-1}^0 \bar{C}_n^{\lambda_1}}{\bar{C}} \frac{2P_a \cdot P_b \bar{d}_{0,n}}{\bar{D}} \right. \\
&\quad \left. + \frac{\bar{\beta}_{\lambda_1} \bar{C}_{\lambda_1-1}^0 \bar{C}_n^{\lambda_1}}{\bar{C}} \frac{\bar{\beta}_{\lambda_2} \bar{C}_{\lambda_2-1}^0 \bar{C}_n^{\lambda_2}}{\bar{C}} \left[\frac{2P_a \cdot P_b \bar{d}_{0,n}}{\bar{D}} + 2 \left(\frac{2P_a \cdot P_b \bar{d}_{0,n}}{\bar{D}} \right)^2 \right] \right\} \\
&\simeq i(P_a \cdot P_b) \int_0^1 d\bar{\alpha}_0 \cdots d\bar{\alpha}_n d\bar{\beta}_1 \cdots d\bar{\beta}_n \delta \left(1 - \sum \bar{\alpha}_j - \sum \bar{\beta}_j \right) \frac{1}{CD} \\
&\quad \times \left(1 - \frac{\bar{\beta}_{\lambda_1} \bar{C}_{\lambda_1-1}^0 \bar{C}_n^{\lambda_1}}{\bar{C}} \right) \left(1 - \frac{\bar{\beta}_{\lambda_2} \bar{C}_{\lambda_2-1}^0 \bar{C}_n^{\lambda_2}}{\bar{C}} \right), \tag{C11}
\end{aligned}$$

where the variable change (5.24) and the identity (5.27) have been used. Equation (C11) agrees with the general expression (5.31). To show (5.32) let us rewrite C_j^l . We define the following matrices:

$$Q_n^0 = \begin{pmatrix} \bar{\alpha}_0 + \bar{\alpha}_1 + \bar{\beta}_1 & -\bar{\alpha}_1 & 0 & 0 & \cdots & \cdot \\ -\bar{\alpha}_1 & \bar{\alpha}_1 + \bar{\alpha}_2 + \bar{\beta}_2 & -\bar{\alpha}_2 & 0 & \cdots & \cdot \\ 0 & -\bar{\alpha}_2 & \bar{\alpha}_2 + \bar{\alpha}_3 + \bar{\beta}_3 & -\bar{\alpha}_3 & \cdots & \cdot \\ 0 & 0 & -\bar{\alpha}_3 & \cdots & \cdots & \cdot \\ \vdots & \vdots & \vdots & \vdots & \vdots & \vdots \\ 0 & 0 & 0 & 0 & \cdots & -\bar{\alpha}_n \\ 0 & 0 & 0 & 0 & \cdots & \bar{\alpha}_{n-1} + \bar{\alpha}_n + \bar{\beta}_n \end{pmatrix}, \tag{C12}$$

Q_{j-1}^0 = a matrix similar to Q_n^0 except that all the lm th elements are replaced by δ_{lm} for $l, m > j-1$,

Q_n^j = a matrix similar to Q_n^0 except that all the lm th elements are replaced by δ_{lm} for $l, m \leq j$,

Q_j = a matrix which differs from the unit matrix only by replacing the j th diagonal element by $\bar{\beta}_j$.

We note that

$$\bar{C} = \det Q_n^0, \quad \bar{C}_{j-1}^0 = \det Q_{j-1}^0,$$

$$\bar{C}_n^j = \det Q_n^j, \quad \bar{\beta}_j = \det Q_j.$$

Then

$$\bar{C}_{j-1}^0 \bar{\beta}_j C_n^j = \det(Q_{j-1}^0 Q_j Q_n^j).$$

It is easy to see that the matrix $Q_{j-1}^0 Q_j Q_n^j$ is similar to Q_n^0 except that the element of the j th column is replaced by $\bar{\beta}_j \delta_{mj}$, $m=1, 2, \dots, n$. This clearly shows that

$$\bar{C} - \bar{C}_{j-1}^0 \bar{\beta}_j C_n^j = (\bar{\alpha}_{j-1} + \bar{\alpha}_j) \bar{C}_{j-1}^0 \bar{C}_n^j + \text{quadratic in } \bar{\alpha}'\text{'s},$$

which is (5.31). We conclude that $I_{\lambda_1 \lambda_2}$ does not contribute to a \ln^{2n} term.

Next we turn to the general case of (5.18). Its integrand contains typical terms such as (5.21). Our problem is to find the number of P terms in it. By (C1) and (C2), we see that a P term does not contain the following products: (a) $(\lambda_j \lambda_j)$, (b) $(j_1 j_3)(j_2 j_3)$ [but $(j_1 j_2)(j_2 j_3)$ is allowed]. Using these rules and examining a few cases, one realizes that the number of P terms in (5.21) can be

found in the following way. We rewrite (5.21) in the form

$$\prod_{j,j'=1}^l \left(\frac{1}{\beta_{\lambda_j}} \mathcal{D}_{\lambda_j}^{\mu_j-1} \mathcal{D}_{\lambda_{j'}}^{\mu_{j'}} \right) e^{iD(a)/C} \Big|_{j'=j} = \sum_{j=0}^l \left(\frac{2i}{C} \right)^{l+j} \{2^{l-j} 1^{2j}\}. \tag{C13}$$

For $j=0$, there is only 1 P term. For $j=1$, the number of P terms is equal to the number of single pairs constructed as follows. Consider two sets of l objects, $\lambda_1, \lambda_2, \dots, \lambda_l$ and $\lambda'_1, \lambda'_2, \dots, \lambda'_l$. A pair, denoted by $(\lambda_j, \lambda_{k'})$, is formed with λ_j from the set $\lambda_1, \dots, \lambda_l$ and λ'_k from the set $\lambda'_1, \dots, \lambda'_l$ and $j < k$. The number of these pairs is

$$S_l^{(1)} = \frac{1}{2} l(l+1). \tag{C14}$$

For $j=2$, the number of two pairs

$$(\lambda_{j_1} \lambda'_{j_2})(\lambda_{j_3} \lambda'_{j_4}), \quad j_1 < j_2, \quad j_3 < j_4, \quad j_2 \neq j'_4, \quad j_1 < j_3$$

is equal to

$$S_l^{(2)} = \frac{1}{24} l(l-1)(l-2)(3l-5). \quad (C15)$$

It is straightforward, though tedious, to general-

ize to $j=3, \dots$. If we denote the number of P terms for the case j by $S_l^{(j)}$, $j \leq l-1$, then (5.22) follows. We remark that $S_l^{(j)}$ is the Stirling number of the second kind.²⁷

*Work performed for the U. S. Energy Research and Development Administration under Contract No. W-7405-eng-82.

†Work supported in part by the National Science Foundation.

¹For a review, see S. Gasiorowicz and D. A. Geffen, *Rev. Mod. Phys.* **41**, 531 (1969).

²S. L. Adler, in *Lectures on Elementary Particles and Quantum Field Theory*, edited by S. Deser, M. Grisaru, and H. Pendleton (MIT Press, Cambridge, Mass., 1971); R. Jackiw, in *Lectures on Current Algebra and its Applications* (Princeton Univ. Press, Princeton, New Jersey, 1972).

³For Reggeization, see M. Gell-Mann, M. L. Goldberger, F. E. Low, E. Marx, and F. Zachariasen, *Phys. Rev.* **133**, B145 (1964); M. Gell-Mann, M. L. Goldberger, F. E. Low, V. Singh, and F. Zachariasen, *ibid.* **133**, B161 (1964); H. Cheng and T. T. Wu, *Phys. Rev.* **140**, B465 (1966); M. T. Grisaru, H. J. Schnitzer, and H.-S. Tsao, *Phys. Rev. Lett.* **30**, 811 (1973); *Phys. Rev. D* **9**, 2864 (1974). For an earlier review, see Hung Cheng and Tai Tsun Wu, in *Proceedings of the 1971 International Symposium on Electron and Photon Interactions at High Energies*, edited by N. B. Mistry (Laboratory of Nuclear Studies, Cornell Univ., Ithaca, New York, 1972). For eikonalization see M. Lévy and J. Sucher, *Phys. Rev.* **186**, 1656 (1969); H. D. I. Abarbanel and C. Itzykson, *Phys. Rev. Lett.* **23**, 53 (1969); S.-J. Chang and T.-M. Yan, *ibid.* **25**, 1586 (1970); G. Tiktopoulos and S. Treiman, *Phys. Rev. D* **3**, 1037 (1971).

⁴S. Weinberg, *Phys. Rev. Lett.* **19**, 1264 (1967); A. Salam, in *Elementary Particle Theory: Relativistic Groups and Analyticity* (Nobel Symposium No. 8), edited by N. Svartholm (Almqvist and Wiksell, Stockholm, 1968), p. 367. For a general review, see for example J. Iliopoulos, in *Proceedings of the XVII International Conference on High Energy Physics, London, 1974*, edited by J. R. Smith (Rutherford Laboratory, Chilton, Didcot, Berkshire, England, 1974), p. III-89. (We shall refer to this proceedings as the London conference.)

⁵D. J. Gross and F. Wilczek, *Phys. Rev. Lett.* **30**, 1343 (1973); H. D. Politzer, *ibid.* **30**, 1344 (1973).

⁶J. Wess and B. Zumino, *Phys. Lett.* **49B**, 52 (1974); A. Salam and J. Strathdee, *Phys. Rev. D* **11**, 1521 (1975).

⁷See Ref. 5. For a review see H. D. Politzer, *Phys. Rep.* **14C**, 129 (1974) and D. Gross, London conference, p. III-65.

⁸S. Weinberg, *Phys. Rev. Lett.* **31**, 494 (1973); also see for example D. Gross, Ref. 7, for a brief review. For bag types of models, see for example A. Chodos, R. Jaffe, K. Johnson, C. B. Thorn, and V. F. Weisskopf, *Phys. Rev. D* **9**, 3471 (1974); M. Creutz, *ibid.* **10**, 1749 (1974); P. Vinciguarelli, *Nucl. Phys.* **B89**, 463

(1975); T. D. Lee and G. C. Wick, *Phys. Rev. D* **9**, 3471 (1974); W. A. Bardeen, M. S. Chanowitz, S. D. Drell, M. Weinstein, and T.-M. Yan, *ibid.* **11**, 1094 (1975).

⁹B. M. McCoy and T. T. Wu, *Phys. Rev. Lett.* **35**, 604 (1975); *Phys. Rev. D* **12**, 3257 (1975).

¹⁰H. T. Nieh and York-Peng Yao, *Phys. Rev. D* **13**, 1082 (1976).

¹¹L. Tyburski, *Phys. Lett.* **59B**, 49 (1975). See also V. S. Fadin, E. A. Kuraev, and L. N. Lipatov, *ibid.* **60B**, 50 (1975).

¹²R. W. Brown, L. B. Gordon, T. F. Wong, and Bing-Lin Young, *Phys. Rev. D* **11**, 2209 (1975).

¹³I. J. Muzinich and H.-S. Tsao, *Phys. Rev. D* **11**, 2203 (1975).

¹⁴C. Lovelace, *Phys. Lett.* **55B**, 187 (1975).

¹⁵J. Cardy, *Phys. Lett.* **53B**, 355 (1974).

¹⁶C. Lovelace, *Nucl. Phys.* **B99**, 109 (1975).

¹⁷E. Abers and B. W. Lee, *Phys. Rep.* **9C**, 1 (1973); J. Iliopoulos and B. Zumino, *Nucl. Phys.* **B76**, 310 (1973); B. Zumino, London conference, p. I-254.

¹⁸See Ref. 6; also see S. Gasiorowicz, Univ. of Minnesota lectures (unpublished).

¹⁹The coupling constant, g , used here in \mathcal{L}_g differs from that defined in Wess and Zumino, Ref. 6, by a factor of $\frac{1}{2}$.

²⁰M. Gell-Mann and M. Lévy, *Nuovo Cimento* **16**, 705 (1960).

²¹P. G. Federbush and M. T. Grisaru, *Ann. Phys. (N.Y.)* **22**, 263 (1963); G. Tiktopoulos, *Phys. Rev.* **131**, 480 (1963); **131**, 2373 (1963).

²²We use $\int_k \equiv (1/2\pi)^4 \int d^4k$. We follow the convention in J. D. Bjorken and S. D. Drell, *Relativistic Quantum Fields* (McGraw-Hill, New York, 1965). However, we use a different normalization for spin wave functions: $\Sigma_s u(Ps)\bar{u}(Ps) = \not{P} + m$ and $\Sigma_s v(Ps)\bar{v}(Ps) = \not{P} - m$. We follow S. Gasiorowicz, *Elementary Particle Physics* (Wiley, New York, 1967), for the charge conjugation of spinor fields.

²³S.-J. Chang and S. K. Ma, *Phys. Rev.* **188**, 2385 (1969).

²⁴S. Blaha, *Phys. Rev. D* **3**, 510 (1971).

²⁵R. J. Eden, P. V. Landshoff, D. I. Olive, and J. C. Polkinghorne, *The Analytic S-Matrix* (Cambridge Univ. Press, Cambridge, England, 1966), pp. 31-36.

²⁶J. D. Bjorken and T. T. Wu, *Phys. Rev.* **130**, 2566 (1963).

²⁷See, for example, John Riordan, *An Introduction to Combinatorial Analysis* (Wiley, New York, 1958), p. 213.

²⁸We would like to thank Dr. B. C. Arnold and Dr. D. Isaacson for a discussion of the derivation of Eq. (5.28).

²⁹A. R. Swift and B. W. Lee, *Phys. Rev.* **131**, 1857 (1963).

³⁰S. D. Drell, D. J. Levy, and T.-M. Yan, *Phys. Rev. Lett.* **22**, 744 (1969).

³¹H. D. Politzer, *Phys. Rep.* **14C**, 129 (1974). However,

it has been pointed out by Nee-Pong Chang, Phys. Rev. D 10, 2706 (1974), that a non-Abelian gauge theory with Higgs scalars can maintain its asymptotic freedom if certain eigenvalue conditions of the renormalization-

group equations are satisfied.

³²B. Zumino, London conference, Ref. 17, p. I-254.

³³C. Ryan and S. Okubo, Nuovo Cimento Suppl. 2, 234 (1964).